

This is to certify that the

thesis entitled

Consolidation and Relaxation Behavior of Continuous Strand Random Glass Mats with Thermoplastic Binders

presented by

John Costain Knight III

has been accepted towards fulfillment of the requirements for

M.S. degree in Chemical Engineering

Date April 8, 1994

MSU is an Affirmative Action/Equal Opportunity Institution

O-7639



LIBRARY Michigan State University

PLACE IN RETURN BOX to remove this checkout from your record. TO AVOID FINES return on or before date due.

DATE DUE	DATE DUE	DATE DUE

MSU is An Affirmative Action/Equal Opportunity Institution cyclecidatedus.pm3-p.1

CONSOLIDATION AND RELAXATION BEHAVIOR OF CONTINUOUS STRAND RANDOM GLASS MATS WITH THERMOPLASTIC BINDERS

by

John Costain Knight III

A THESIS

Submitted to
Michigan State University
in partial fulfillment of the requirements
for the degree of

MASTER OF SCIENCE

Department of Chemical Engineering

ABSTRACT

CONSOLIDATION AND RELAXATION BEHAVIOR OF CONTINUOUS STRAND RANDOM GLASS MATS WITH THERMOPLASTIC BINDERS

By

John Costain Knight III

The consolidation and relaxation characteristics of continuous strand random glass mats containing thermoplastic binders were studied. An instrumented hydraulic press was used to compress the mats over a range of temperatures (51.7°C - 176.7°C) and platen closing speeds (0.02 mm/sec - 2.00 mm/sec). The binder viscosity was seen to be a strong function of temperature and strain rate. Scanning electron microscopy was used to examine deformations of individual fiber tows.

As the temperature is increased, the pressure required during consolidation is decreased, and the final fiber volume fraction is increased. At moderate closing speeds, the compaction pressure is increased with increasing speed, but at the highest speed the pressure decreased and the mats behaved more like aligned fibers. Mat relaxation was increased with increasing temperature, but varying the closing speed had no effect. The fiber tows were observed to flatten during consolidation, more so at high temperatures and low closing speeds.

For Beth, Agatha, and Sassafras

ACKNOWLEDGEMENTS

The author wishes to thank: Dr. K. Jayaraman for suggesting this topic and providing guidance and support during the project; Jack and Sandy Knight for providing guidance and support all my life; and Rob Polance for providing valuable assistance with equipment and paying me to wear polyethylene extrudate on my head.

This research was supported by the State of Michigan through an REF grant administered by the Composite Materials and Structures Center at Michigan State University, and in part by the NSF Research Center for Polymer Composites Processing at Michigan State University.

TABLE OF CONTENTS

<u>Pa</u>	age
List of Tables	.vi
List of Figures	vii
Chapter 1. Introduction	1
Chapter 2. Experimental	.12 .12 .15 .16 .16
Chapter 3. Results and Discussion. 3.1. Binder Characterization Results. 3.2. Mat Consolidation Results. 3.2.1. Varying Maximum Pressure Setting. 3.2.2. U-816 Consolidation Results. 3.2.3. U-750 Consolidation Results. 3.3. Mat Relaxation Results. 3.4. Scanning Electron Microscopy Results.	.25 .29 .29 .33 .33
Chapter 4. Modelling	.60
Chapter 5. Summary and Conclusions	.66
Chapter 6. Recommendations	.68
Appendix A: Sample Calculations	.71
List of References	72

LIST OF TABLES

Tak	<u>Page</u>
1.	Shift factors for U-750 binder27
2	Relaxation of U-750 glass mat stacks, %47
3 .	Relaxation of U-816 glass mat stacks, %47
4 .	Average width of U-750 fiber tows after deformation57
5.	Apparent number of U-750 fiber tows in mat thickness before and after consolidation58
6.	Gutowski model parameters, U-750 mat61
7.	Batch and Macosko model parameters, U-750 mat62
8.	Batch and Macosko model parameters, U-816 mat62
9.	Batch and Macosko model parameters, varied maximum pressure on U-750 mat63

LIST OF FIGURES

Figu	<u>re</u> <u>Page</u>
1.	Expected consolidation behavior of random mats and aligned fiber rovings [8]
2.	Wabash hydraulic press and accessories13
3.	Pressure and gap height transients as recorded on a strip chart recorder21
4.	Differential scanning calorimetry run on U-750 binder26
5.	Master curve for viscosity of U-750 binder (T _{ref} = 93°C)28
6.	Arrhenius plot of shift factor for U-750 binder $(T_{ref} = 93 ^{\circ}\text{C}, \text{ Activation energy} = 85 \text{KJ/gmol}) \dots 30$
7.	Effect of increasing maximum pressure on consolidation behavior of an eight-ply stack of U-750 at 93.3°C32
8.	Consolidation behavior of an eight-ply stack of U-816 at 0.85 mm/sec34
9.	Consolidation behavior of an eight-ply stack of U-750 at 0.02 mm/sec
10.	Consolidation behavior of an eight-ply stack of U-750 at 0.15 mm/sec
11.	Consolidation behavior of an eight-ply stack of U-750 at 0.85 mm/sec
12.	Consolidation behavior of an eight-ply stack of U-750 at 2.00 mm/sec
13.	Consolidation behavior of an eight-ply stack of U-750 at 51.7°C mm/sec40
14.	Consolidation behavior of an eight-ply stack of U-750 at 93.3°C41

Figu:	<u>re</u>							Pa	ge
20.	Average	thickness	of	U-750	fiber	tows	after		
	consolid	lation							56

CHAPTER 1

INTRODUCTION

1.1. Background

In general, composites are a class of materials which are formed by the combination of two or more materials into a single two-phase material: a matrix material such polypropylene, and a reinforcing material such as glass fibers. Both the composite matrix and reinforcement may be either metal, ceramic, or polymer. Reinforcement or matrix materials are chosen to make the resulting composite stronger, tougher, more durable, more heat-resistant, lighter, or more rigid than the matrix alone. A good example of a composite material is road concrete: the addition of steel reinforcing rods embedded in the concrete makes the road stronger and more resistant to damage caused by frost. Especially within the thirty years, composite materials have become past commercially important; consumers may be familiar with carbon or boron fiber tennis rackets or sheet molding compound in their automobile fenders and bumpers. Other areas where have become increasingly important composites aerospace, the military, and construction. One of the most common types of composite is the polymer matrix / glass fiber reinforcement system. A wide variety of such systems are commonly used: the polymer may be either thermoplastic or thermosetting; the fibers may be chopped or continuous, aligned or random, with or without a binder.

Consider such a composite system with a thermosetting resin and a continuous strand, random, binder-coated glass fiber mat reinforcement. A common step in the manufacture of such a composite is consolidation of the fibers. For instance, in injection molding, the fiber preform may be subject to a process called thermoforming, in which a fiber reinforcement stack is heated and compressed in a compression tool to achieve a particular fiber volume fraction. The preform is then removed from the tool, at which time it relaxes or lofts, and transferred to a mold before the resin is introduced. The proper relationship between compression force and fiber volume fraction is thus of interest to composite materials processors, as is the relationship of the fiber mat relaxation behavior processing consolidation and to conditions.

Processing of the composite may be affected by the presence of a binder in any of several ways. The distribution of the binder after consolidation may affect how the binder is dissolved and washed out by the injected resin. Large amounts of dissolved binder in the resin may affect mechanical properties of the finished composite. Similarly, binder dissolution into the injected resin can locally alter the viscosity of the resin, which can lead to fingering, a phenomenon in which a higher density fluid (resin with binder) displaces a lower density fluid (resin with less binder). Fingering also may affect the mechanical properties of the finished composite. Finally, during the consolidation process,

the temperature and squeezing rate will affect the viscosity of the binder. For instance, at higher temperatures the lower binder viscosity may cause it to act as a lubricant, plus the viscosity may be lowered further at fast squeezing rates if the binder exhibits shear-thinning behavior. The effect of varying viscosity of a polymeric binder on the load / deformation behavior of continuous strand random mats is the issue addressed in this paper.

1.2. Literature Review

Much of the previous work in fiber consolidation was done as part of an attempt to model fiber deformation and resin flow in the processing of composites. The following model was established by Gutowski and co-workers [1-7]:

$$\sigma = A_s \frac{\sqrt{\frac{V_f}{V_o}} - 1}{(\sqrt{\frac{V_a}{V_f}} - 1)^4}$$

to model the consolidation of an aligned fiber network. In this model, V_f is the fiber volume fraction, V_a is the maximum allowable fiber volume fraction, V_o is the initial fiber volume fraction, A_a is a constant dependent on the bending stiffness and span-length-to-height ratio of the fiber network, and σ is the stress (pressure) supported by the fiber network. This model is based on the assumption that at low fiber volume fractions, the fibers do not carry any of the load because there are very few fiber-to-fiber contact points.

As V, increases, the waviness and misalignment of the fibers establish more and more fiber contact points until a fiber network is established, and the fibers can carry a rapidly increasing load. Eventually, the fibers will be compressed to the point where a maximum allowable fiber volume fraction is approached, and the pressure required to compress the fibers infinity. further diverges to This model was successfully to data on well-aligned and poorly-aligned fiber systems. In later work [2-4] dealing with permeability of fiber systems, Gutowski studied the compaction of aligned fibers fully impregnated with oils of different viscosities (organic oil, 0.05 Pa-s; castor oil, 0.91 Pa-s; and silicone oil, 9.62 Pa-s) and examined the load/deformation behavior. The closing speeds used were very low (0.002 - 0.005 in/min) and the samples were confined. He found that the oil pressure in the system was rarely greater than 5% of the applied pressure, indicating that the fiber network was supporting the bulk of the load. The effect of the oil viscosity on the consolidation characteristics of the fibers was not the focus of the study, and thus no results of this type were given. Gutowski later expanded his model to allow for threedimensional resin flow and 1-dimensional fiber deformation [4-5] and to study the response of a lubricated fiber bundle to 3-dimensional stresses [6].

Batch and Macosko [8] recognized that the deformation behavior of random mats and aligned fiber rovings must be different (Figure 1) because of different amounts of fiber-to-

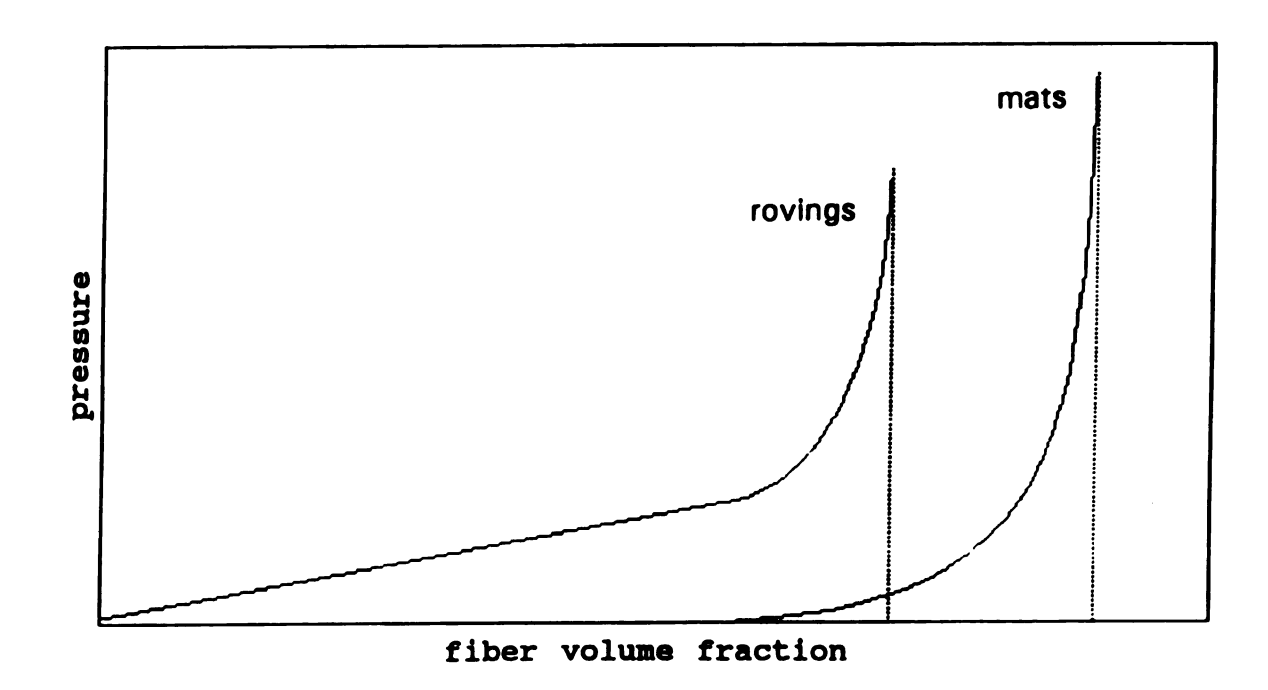


Figure 1. Expected consolidation behavior of random mats and aligned fiber rovings [8].

fiber contacts. They proposed a two-stage model for fiber deformation, which is applicable to both random and aligned fibers. This model is similar in concept to Gutowski's in that it models a single fiber being compressed inside a rigid cell as a representation of the entire mat. In their model, the fiber mat network is assumed to behave as a Hookean solid at low fiber volume fractions during the first stage:

$$P=K_{o}(V_{f}-V_{o})$$

in which P is pressure and K_o is the "spring constant" of the mat. At some point a transitional volume fraction $(V_{f,cont})$ is reached, more fiber-to-fiber contacts are established, and the second stage, that of non-Hookean behavior, begins:

$$P = \frac{K_o}{\left(1 - \frac{m}{m_m}\right)} \left(V_f - V_o\right)$$

in which m is the length of the fiber-to-fiber contact, m_{∞} is the maximum contact length, and the other parameters are as defined previously. In the equation above, the quantity m/m_{∞} is defined as

$$\frac{1 - \left[\frac{\frac{1}{V_o} - \frac{1}{V_{\infty}}}{\frac{1}{V_o} - \frac{1}{V_f}}\right] h}{\frac{m}{m_{\infty}} = \frac{1 - \left[\frac{1}{V_o} - \frac{1}{V_f}\right] h}{1 - h}$$

in which the parameter h (0 < h < 1) is called the packing inefficiency. h will have a low value for aligned fibers and will be higher for random mats or poorly-aligned fibers.

Although Batch and Macosko did not report on any of their own fiber consolidation experiments, they found good agreement between published data and their model for aligned fiber systems. However, the data they used for consolidation of random mats were only in the low fiber volume fraction range, so they only applied the first model stage to them.

In their work, Batch and Macosko also described an empirical model developed by Hou [9], based on a finitely extendable nonlinear elastic (FENE) spring model for the fibers. This model is similar in appearance to Gutowski's, except that it includes a fourth parameter which can be adjusted to fit compression force to both aligned and random fibers:

$$P_{f} = A_{FENE} \frac{(1 - \frac{V_{o}}{V_{f}})}{(1 - \frac{V_{o}}{V_{f}})^{n}}$$

$$[1 - \frac{(1 - \frac{V_{o}}{V_{f}})}{(1 - \frac{V_{o}}{V})}]^{n}$$

In this model, V_o and V_f are as defined in Gutowski's model, V_∞ is the same as V_a , and A_{FENE} and n are constants. However, because this model is empirical, A_{FENE} and n have no physical meaning.

Kim, McCarthy, and Fanucci [10] studied the response of dry reinforcement materials to compressive forces to predict fiber compressibility in a pultrusion die. They found that the load/deformation behavior was strongly dependent on both the fiber orientation (i.e., unidirection, bidirection,

combination) and the stacking methods (i.e., aaabbb, ababab) used. They also found differences between the behavior of dry reinforcements and prepreg samples. They recognized that the maximum fiber volume fraction V_a is a characteristic of the fiber preform, and that the value for lubricated fiber bundles is different from the value for dry fiber bundles. They made no attempt to derive their own model, although they were able to fit Gutowski's model to their data. They also reported that a model proposed by Taylor [11], working in the field of soil mechanics, is also applicable to a fiber network:

$$V_f = V_1 + C_c \log_{10} \left(\frac{\sigma}{\sigma_1} \right)$$

in which σ_1 is taken as 1 MPa, V_1 is the fiber volume fraction when the stress is equal to 1 MPa, and C_c is a constant of the system called the compression index, which is a measure of how much compression will take place. σ_1 is taken as 1 MPa because that is the approximate point where the stress begins rising rapidly, and thus it is a measure of how compliant the mat is at the start of compression.

Knight and Jayaraman [12] presented some preliminary data examining the effects of varying the compression temperature and closing rate on the consolidation characteristics of random glass mats with binders. The trends seen were that as temperature increased, the compressibility of the mats was increased, shown by a decrease in pressure required to obtain a certain fiber volume fraction. Similarly, an increase in closing rate was found to decrease pressure as well. Also, by

comparing compression runs performed at room temperature and at the onset of binder melting, it was shown that at and below the binder melting point, temperature has no effect on the consolidation characteristics of the mat.

Piechowski and Kendall [13] studied the effects of closing speed, temperature, the number of layers of glass mat, and dwell time at full compression on the compressibility and relaxation of random continuous strand E-glass mat. A statistical approach to determining the effect of each variable was taken, with the compression modelled with an equation of the form

$$y = \beta_0 + \beta_1 x_A + \beta_2 x_B + \beta_3 x_D + \beta_4 x_{AB} + \beta_5 x_{AD} + \beta_6 x_{BD}$$

in which y is the pressure, the betas are regression coefficients and x_A , x_B , x_D , x_{AB} , x_{AD} , and x_{BD} are coded variables representing closing speed, platen temperature, number of layers, and their respective interactions. Relaxation of the mats was considered to be the ratio of the mat stack height after processing to the stack height before processing. The relaxation was modelled statistically, similarly to consolidation, with

$$y = \beta_0 + \beta_1 x_B + \beta_2 x_D + \beta_3 x_{BD}$$

in which the variables are the same as defined above. In their statistical study, Piechowski and Kendall determined that the variability in compression characteristics of glass mats is a result mainly of closing speed (63%). The next most significant effects are of interactions between closing speed

and temperature (8%) and closing speed and the number of layers of mat (6%). The conclusion from these results is that at low closing speed, compaction pressure and its variability are lower, and independent of temperature and number of layers. The effect of temperature was found to have only a 2.5% significance to variability of compaction pressure. For relaxation, their conclusions were that low temperatures reduced relaxation, the number of layers had a much less significant effect than temperature, and closing speed and dwell time had very small effects.

There have been several other studies which were not directly related to the subject of fiber consolidation, although the authors touched on it in their work. Davis and McAlea [14] studied the load/deformation behavior of glass mat reinforced thermoplastics (GMTs) in squeezing flows. Their procedure involved heating a precut GMT on their platens and allowing the fiber network to loft, then squeezing it back to its original thickness, waiting for thermal equilibration, then squeezing the GMT to about half of its original thickness. Their results showed a load/deformation curve in three parts: void reduction and resin squeeze-out, composite flow, and load decay. In a study to determine the effects of mat consolidation due to pressure applied by resin in injection molding, Trevino et al. [15] characterized both the permeability and compressibility of fibrous mats. He observed that the porosity of random fiber mats decreased from about 95% to about 60% when a pressure of 1 MPa was applied, and that the porosity of random mats was significantly higher than directional fibers. He used a logarithmic model similar to Taylor's to model deformation. Among his conclusions were that the mats revealed a viscoelastic type response to pressure, and closing speed may thus be an important factor in determining the peak pressure during compression.

1.3. Objectives

There have been a number of studies on the consolidation behavior of aligned [1-7] and random [7-10,12-15] glass reinforcing materials and on fiber mat relaxation [10,13], but as yet there has been no study on the effect of the viscosity of a binding material surrounding a reinforcement on its consolidation and relaxation characteristics. The specific objectives of this study are:

- 1. To study the consolidation and relaxation behavior of continuous strand random glass mats over a broad range of temperatures (51.7°C to 176.6°C) and closing speeds (0.02 mm/sec to 2.00 mm/sec) to determine the trends in such behavior with changing binder viscosity;
- 2. To examine the processed glass mats under scanning electron microscopy to determine the relationship, if any, between the consolidation behavior of the mats and of the individual fiber tows;
- 3. To use an existing model for fiber consolidation to observe how the model parameters are affected by changing binder viscosity.

CHAPTER 2

EXPERIMENTAL

2.1. Materials

Two types of random glass mat were used: one with a polyester binder that is not thermoformable and has low solubility in styrene (Vetrotex / CertainTeed U-816) and one with a polyester binder which has a moderate solubility in styrene and is thermoformable (Vetrotex / CertainTeed U-750). Both mat types are manufactured by allowing fiber tows to fall from a nozzle onto a conveyor in a winding pattern while binder is sprayed on the forming mat. The process leads to anisotropy; the mats are random in the x-y plane but are aligned in the z-direction. The fiber tows themselves are made of many small fibers wound together. Both of these mats, as well as the binder itself in powder form, were obtained through the courtesy of Mr. David Hoyer and Mr. Bob Carvalho of Vetrotex / CertainTeed. It should be noted that the binder constituted only eight weight percent of the mat, and at no time did it fill all the voids in the mat.

2.2. Equipment

2.2.1. Hydraulic press and accessories

An instrumented Wabash hydraulic press (Figure 2) was used to perform the consolidation experiments. The press had one stationary platen (top) and one movable platen, or ram (bottom). Operation of the press was controlled by a timer,



Figure 2. Wabash hydraulic press and accessories.

two switches with adjustable actuators, and several pushbuttons. A pressure transducer measured the pressure in the press' hydraulic fluid. Two thermocouples, one beneath each platen, measured the temperatures of the upper and lower platens. Controls on the press allowed one to set the maximum pressure, closure rate, upper and lower platen temperatures, and cooling water flow through the platens.

The two adjustable actuators controlled the closure of the ram by activating two switches. One of the switches (cycle reset) shut the press off when the ram was opened fully, the other switch (slowdown adjustment) caused the ram to assume the preset constant closure rate. The operating cycle of the press was as follows: when closure was started, the ram would close rapidly until the second (top) switch was actuated, then assume the preset closure rate. The point at which this happened is called the slowdown point. A slowdown point is included in the press operating cycle so an initial gap height may be set.

A sliding linear motion potentiometer was attached to the stationary platen, with the slider attached to the ram. With it, the gap height between the upper and lower platens could be monitored continuously. Electrical potential was supplied to the potentiometer by an external five-volt power source. The potentiometer, pressure transducer, and platen thermocouples all were equipped for connection to a two-channel strip chart recorder. The first channel on the recorder was connected to the potentiometer and the second

channel was connected to the pressure transducer, so pressure and gap height data would be recorded simultaneously throughout the compression experiments.

2.2.2. Other equipment

A Rheometrics RMS-800 rheometer was used to study the viscosity behavior of the binder. To measure the viscosity of some polymeric material, a solid disk of the polymer is held between two flat parallel circular plates, either 25 mm or 50 mm in diameter, which are attached to an upper and a lower test fixture. The gap between the plates is measured very precisely. The rheometer is equipped with an environmental chamber, so the test fixtures and the polymer can be held at a specified elevated temperature. The upper plate is held steady while the lower one rotates (to determine steady shear viscosity) or oscillates (to determine complex viscosity) at a fixed rate or frequency. Viscosity is determined by the machine by measuring the amount of torque on the top plate.

To examine pieces of the processed glass mat, a JEOL JSM-35C scanning electron microscope was used. An SEM produces magnified topographical images of a sample by rastering an electron beam across a selected area of the sample very rapidly. Secondary electrons are emitted from the sample due to inelastic interactions between electrons in the beam and electrons in the sample. These secondary electrons are collected by a detector. At each point in the raster, a computer analyzes the number of secondary electrons and places

a dot on a viewing screen, the brightness of which depends on the number of secondary electrons. The amount of secondary electrons reaching the detector is affected by the topography of the sample; therefore the dots in the image on the screen make a 3-dimensional image. One dot is placed on the screen for every point in the raster; a complete raster fills the screen with dots. Photomicrographs are produced by photographing the screen with an attached Polaroid camera and Polaroid 665 film.

2.3. Procedure

2.3.1. Binder Characterization

The thermal characteristics of the binder were determined using differential scanning calorimetry (DSC). In DSC, a sample of the polymer and a blank reference are maintained at the same temperature throughout a temperature ramp. The difference between the heat added to the sample and the heat added to the reference while keeping their temperatures the same is plotted against temperature. The plot reveals thermal transitions in the sample such as melting points, glass transitions, and heats of reaction.

To determine the viscosity behavior of the binder on the RMS-800, it first was necessary to produce solid discs of the binder 1-2 mm thick and at least 25 mm in diameter. The platens in the press were heated to 93.3°C. A small amount of the powdered binder was placed in the press between two sheets of mold release film. After the binder had been allowed to

melt, the press was started and the platens allowed to travel until they were 1-2 mm apart, which cast the melted binder into a disc. The platens were then cooled to room temperature and the disc of binder was removed for rheological testing. Several of these discs were made. Rheological testing was done in the Rheometrics RMS-800 following the procedure outlined in the manual. Dynamic testing was done at 93°C, 122°C, 136°C, and 176°C at frequencies between 0.01 and 100 rad/sec.

2.3.2. Mat Consolidation

Calibration of the linear motion potentiometer ("pot") attempted as a first step in the consolidation experiments. The ram was opened as far as was possible without damage to the pot, and the switch actuator was positioned to stop the ram there. This was done as a precaution to avoid equipment damage; the ram was rarely opened that far during the experiment. The power source was turned on and the pot was connected to the strip chart recorder. The settings on the recorder were then adjusted so that the pen recording the gap height was at the top of the paper. The platen gap height and the pen position were then recorded. The ram was then closed in small increments, with the gap height and pen position recorded at each point, until it was completely closed. A plot of gap height versus pen position was then prepared and the data points were fit by linear regression. This was done at each intended processing temperature. However, it was found that the plots generated this way were not reproducible and

did not vary with temperature in a predictable way. The slopes of the lines varied very little, but the y-intercepts varied considerably and seemingly randomly. The reason for this is not known but it is suspected that there may be a defect in the power source which causes small variations in voltage output. For this reason, standard calibration plots were not used in these experiments; instead, a two-point calibration was performed during each experimental run as follows: before beginning any experimental runs, the gap height at the slowdown point was measured by setting the closure rate knob to zero, which caused the platens to stop moving at the slowdown point. The platens were then moved to the slowdown point, and the gap height was measured. The compression experiment was then performed, and the gap height at maximum pressure was measured. The two measured gap heights were then matched to their respective line positions on the strip chart: the slowdown point is where there is a knee in the curve, and the maximum pressure point is where the curve levels off at the end of the run.

Calibration of the pressure curve was done in the same way; it was found that the voltage output from the pressure transducer was proportional to pressure, so two-point calibration was performed during each experimental run: the pressure at the beginning of the run and at the end of the run were recorded along with the respective pen positions and linear interpolation was used for each point in between.

To perform the actual consolidation experiments, the

press was prepared by selecting a closing rate and platen temperature and setting the controls accordingly. Eight 4-inch by 4-inch squares of the glass mat were cut from the roll and stacked together, forming a stack about 40 cm high. These consolidation experiments were conducted on a stack of the mat, instead of a single piece, because a stack provides greater platen separation for any given fiber volume fraction and also increases the amount of platen travel necessary to increase the fiber volume fraction. Thus, pressure does not build up as fast as with a single piece of mat, and the strip charts are easier to read. A stack was also used to simulate actual industrial thermoforming processes, which use mat stacks.

The stack was placed on the lower platen in the press between two pieces of mold release film, used to prevent the binder from sticking to the platens. The platens were brought together so that both platens touched the stack surfaces and the stack was allowed to heat to platen temperature over a period of several minutes. When the stack had been heated long enough, the strip chart was started and the consolidation process was begun. The lower platen moved upwards at the preset closure rate. During the time the platens were moving together, but before much pressure had built up, the pressure reading was written on the strip chart by the channel 2 pen, for the first calibration point. At this point the force exerted by the press was about 0.35 tons, which is the force required to raise the ram. The pressure reached the maximum

preset level when the mat stack had been squeezed to roughly 3 mm thick. After the pressure had reached its maximum, the third potentiometer calibration point was obtained (see above) and the pressure was noted by the pen on the strip chart recorder, so the second calibration point for the pressure calibration can be obtained. The pressure was then released, and the recorder stopped. A typical strip chart from such an experiment is shown in Figure 3. The raw chart data obtained from such a chart was converted to pressure and gap height by comparison with calibration curves, and the data was then converted to pressure and fiber volume fraction (see sample calculation, appendix A).

followed for above procedure was the (thermoformable) mats at squeezing rates of 0.02 mm/sec, 0.15 mm/sec, 0.85 mm/sec and 2.00 mm/sec and at temperatures of 51.7°C, 93.3°C, 135.0°C and 176.7°C. For the U-816 (nonthermoformable) mats, the procedure was followed with a squeezing rate of 0.85 mm/sec at the same temperatures. Varying the squeezing rate was not done on the U-816 mats because they were considered only controls for temperature variations in the other mats, since the low solubility binder is not thermoformable. To verify that the maximum pressure does not affect the consolidation characteristics of the mat, the above procedure was followed in several experimental runs in which temperature and closure rate were kept constant but the maximum pressure was changed. A closing speed of 0.85 mm/sec and a temperature of 121.1°C were used, with the

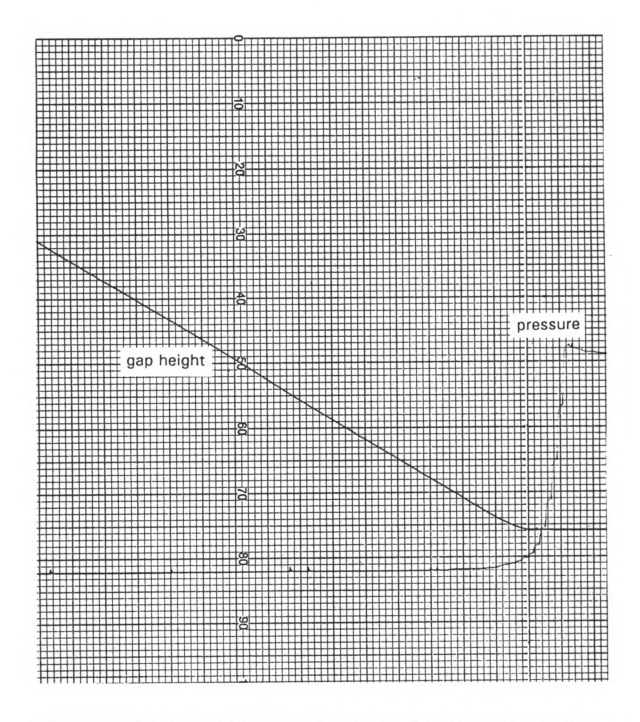


Figure 3. Pressure and gap height transients as recorded on a strip chart recorder.

maximum pressure varying between 0.75 and 16 MPa.

2.3.3. Mat Relaxation

Relaxation is determined by compressing a stack of glass mat in the press the same way as in the consolidation experiments, then releasing the pressure after a certain "dwell time" at maximum pressure. The stack is then removed from the platens and allowed to cool to room temperature on a flat bench top. Relaxation is defined here as the ratio of the height recovered after compression to the height lost during compression, or

$$R = \frac{h_f - h_c}{h_o - h_c} \times 100\%$$

in which h_o is the original height of the stack, h_c is the height of the stack while under full compression, and h_f is the final stack height after pressure is released. A number of both U-750 and U-816 mat stacks were prepared and compressed the same way as in the consolidation experiments, and each was tested for relaxation by leaving the stacks pressed at maximum pressure for 30 seconds, then releasing the pressure, removing the stacks from the press, and allowing them to cool. After they had cooled, the thickness of each stack was measured, using a ruler, at eight points around its perimeter. The height of the stack was taken to be the average of the measurements. Relaxation experiments were carried out using closing speeds of 0.85 mm/sec and 2.00 mm/sec and temperatures

of 51.7°C, 93.3°C, 135.0°C, and 176.7°C for both kinds of mat.

2.3.4. Scanning Electron Microscopy Study

To observe what happens to the mats and binder during the consolidation process on the scale of single fibers, scanning electron microscopy (SEM) was used. Eight glass mat stacks were prepared in the same way as described above, except that in this case, teflon mold release film was used as a liner between the mats and the platens, and the platens were cooled to room temperature while maximum pressure was applied to the mats. By cooling the platens, the binder was allowed to resolidify within the preform and form a hard, unlofted plaque which retained the thickness of the mats and the fiber configuration at maximum consolidation. The teflon film did not adhere to the mats, so the surface of the resulting plaque would not be disturbed by removing it. The plaques intended for SEM study were preformed at conditions of 0.02 mm/sec and 2.00 mm/sec closing speeds, each closing speed done at 51.7°C, 93.3°C, 135.0°C, and 176.7°C. A 1-cm square piece was cut from each plaque as carefully as possible using a razor blade. Each piece was then cemented onto an SEM mounting stub using epoxy cement. Since SEM does not work well with a non-conductive sample, each mounted piece of glass mat was coated with gold in a sputter coater for three times for two minutes a time, tilting the stub and rotating it in between each coating so each face of the sample was coated. When the samples had thus been made conductive, they were placed inside the sample chamber and examined one by one, using a 20 kilovolt accelerating voltage, a #2 aperture, and 20x magnification. A Polaroid camera attached to the SEM was used to obtain photomicrographs of each plaque sample. A photomicrograph was also taken of the undeformed glass mat.

CHAPTER 3

RESULTS AND DISCUSSION

3.1. Binder Characterization Results

A DSC run on the binder is shown in Figure 4. The binder is seen to have a melting range of 50-65°C with a peak at 58.26°C. The peak temperature may be considered the melting point of the binder. The heat of fusion, calculated by integration, is 10.97 J/g.

The rheological data for the binder was obtained at the four different temperatures, and time-temperature superposition [16] was applied to it. The family of curves obtained by plotting viscosity against shear rate on a log-log plot at several temperatures has roughly the same shape, but each curve has a different position. In time-temperature superposition, all the curves can be made to superpose with a curve at a reference temperature (T_{ref}) by shifting each curve at temperature T $(T \ge T_{ref})$ upwards and to the right by the equal amounts, given by the "shift factor," a_T :

$$a_{T} = \frac{\eta_{o}(T) T_{ref} \rho_{ref}}{\eta_{o}(T_{ref}) T \rho} \approx \frac{\eta_{o}(T)}{\eta_{o}(T_{ref})}$$

The shift factor is the amount that each curve must be shifted upwards and to the right to superpose it with the reference curve, and is approximately equal to the log of the ratio of the zero-shear viscosity at $T_{\rm ref}$ to the zero-shear viscosity at

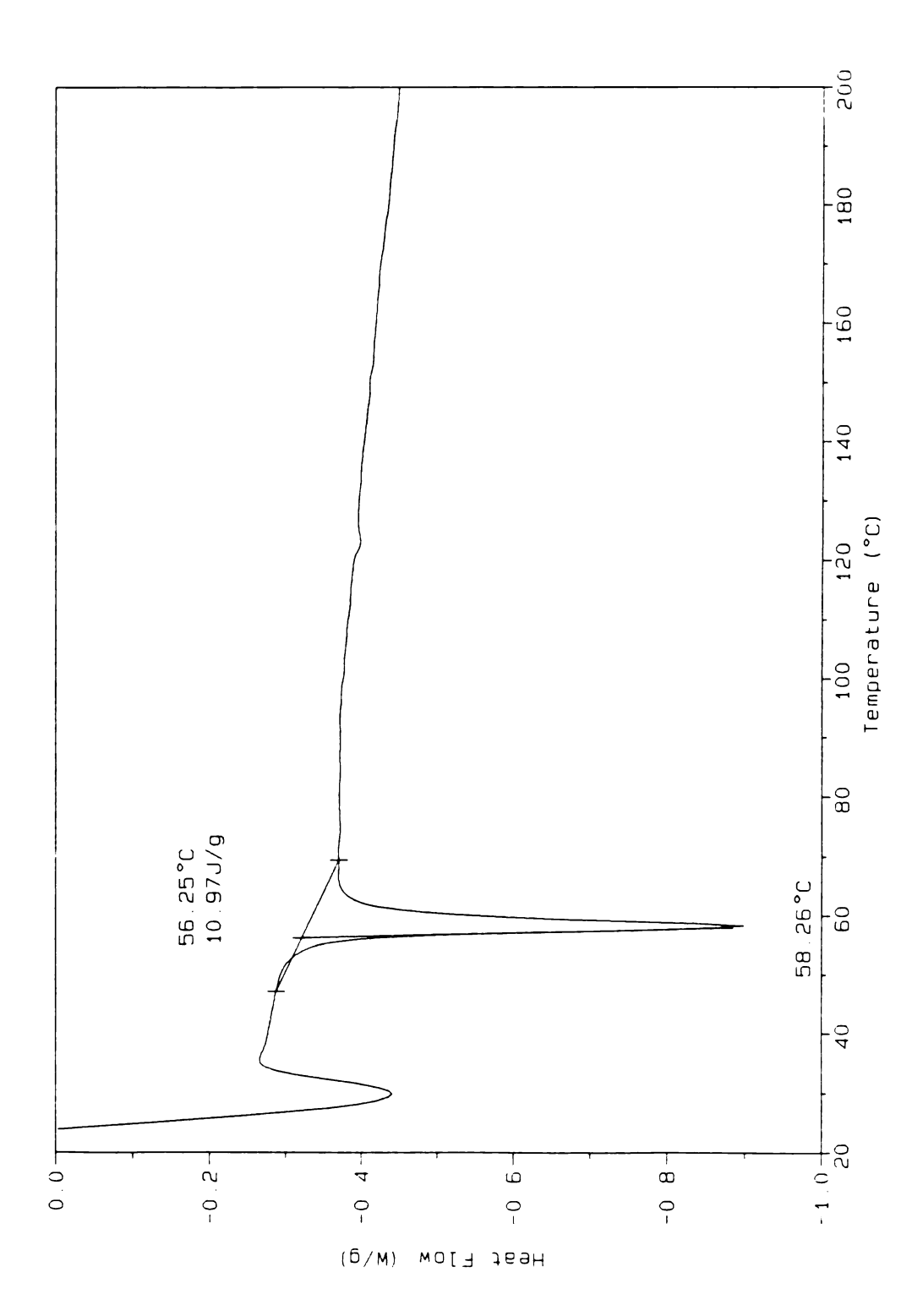


Figure 4. Differential scanning calorimetry run on U-750 binder.

T. Using the shift factor, reduced properties are obtained, which superpose when plotted. The reduced properties are given by

$$\eta_r = \frac{\eta (\dot{\gamma}, T) T_{ref}}{a_r T}$$

and

$$\omega_r = a_T \omega$$

In which η and η_r are the viscosity and reduced viscosity, respectively, and ω and ω_r are the frequency and reduced frequency, respectively. By plotting the reduced properties for each temperature, one can obtain a master curve for the viscosity. The shift factors were found for temperatures of 122°C, 136°C, and 176°C with a reference temperature of 93°C, and from these the reduced viscosities and frequencies were determined. The shift factors are summarized in Table 1, and the master curve is shown in Figure 5.

Table 1. Shift factors for U-750 binder.

Temp, °C	Shift factor		
93	-		
122	0.107		
136	0.0285		
176	0.00422		

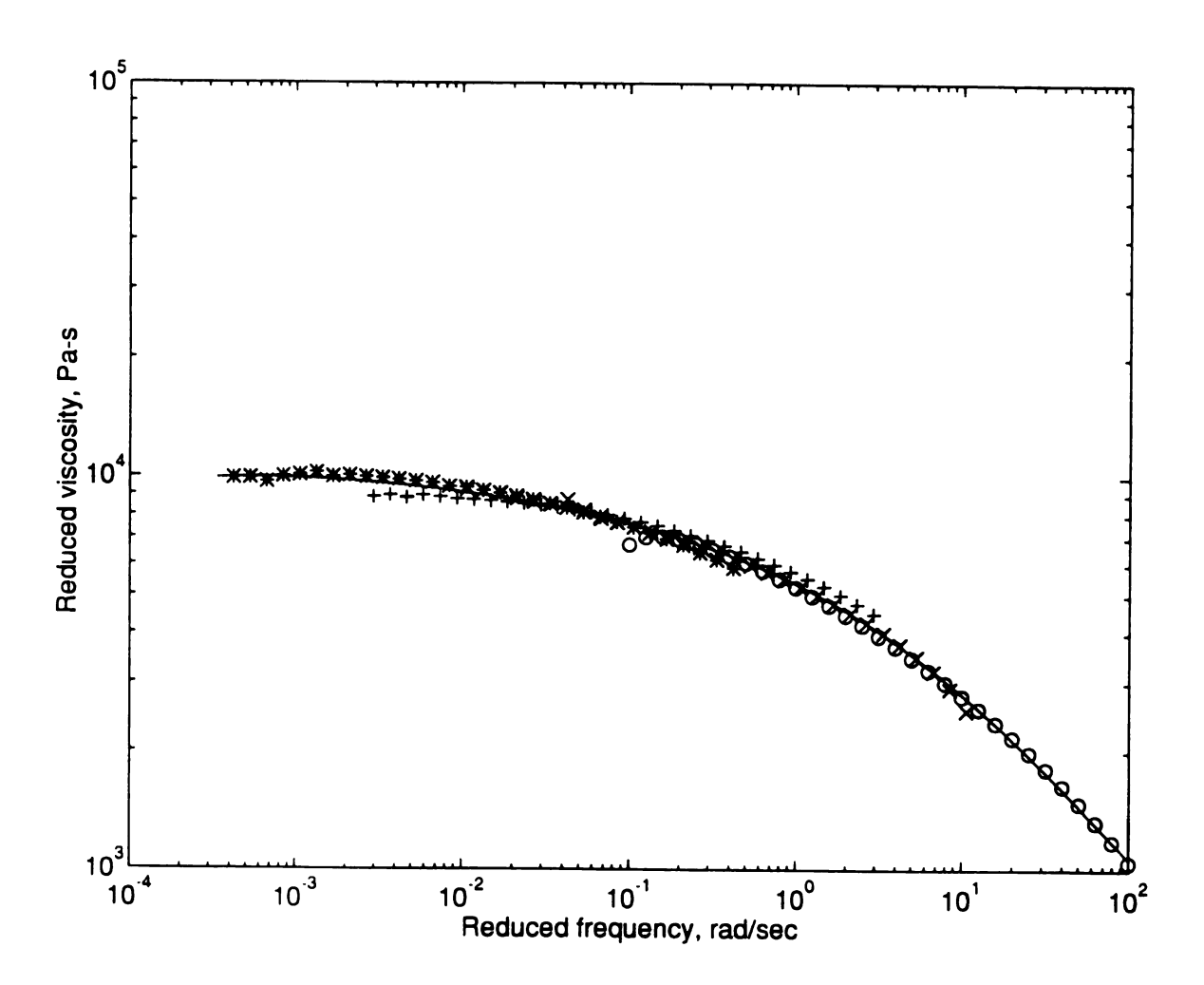


Figure 5. Master curve for viscosity of U-750 binder ($T_{ref} = 93\,^{\circ}\text{C}$).

The shift factors can be described by an Arrhenius relationship [16]:

$$\log a_T = \frac{E_{\eta}}{R} \left(\frac{1}{T} - \frac{1}{T_{ref}} \right)$$

In which a_T is the shift factor, E_η is the activation energy for flow of the polymer, R is the universal gas constant, T is the absolute temperature, and T_{ref} is the absolute reference temperature. In this work, the reference temperature was chosen to be 93°C (366 K). An Arrhenius plot of the shift factor is shown in Figure 6. From the slope of the best-fit curve, the activation energy for the U-750 binder was determined to be 85 KJ/gmol.

3.2. Mat Consolidation Results

3.2.1. Varying Maximum Pressure Setting

The first set of fiber consolidation experiments involved varying the preset maximum pressure to determine whether or not the maximum pressure had any effect on the consolidation curves. A closing rate of 0.85 mm/sec and a platen temperature of 93.3°C were arbitrarily chosen, and ten roughly equally spaced pressure settings between 0.75 MPa and 16 MPa were chosen. Forty stacks of the medium solubility binder mat were prepared and the experimental procedure was carried out as described previously. Four runs were performed at each pressure setting, keeping the temperature and closing rate constant. The four pressure transients obtained for each

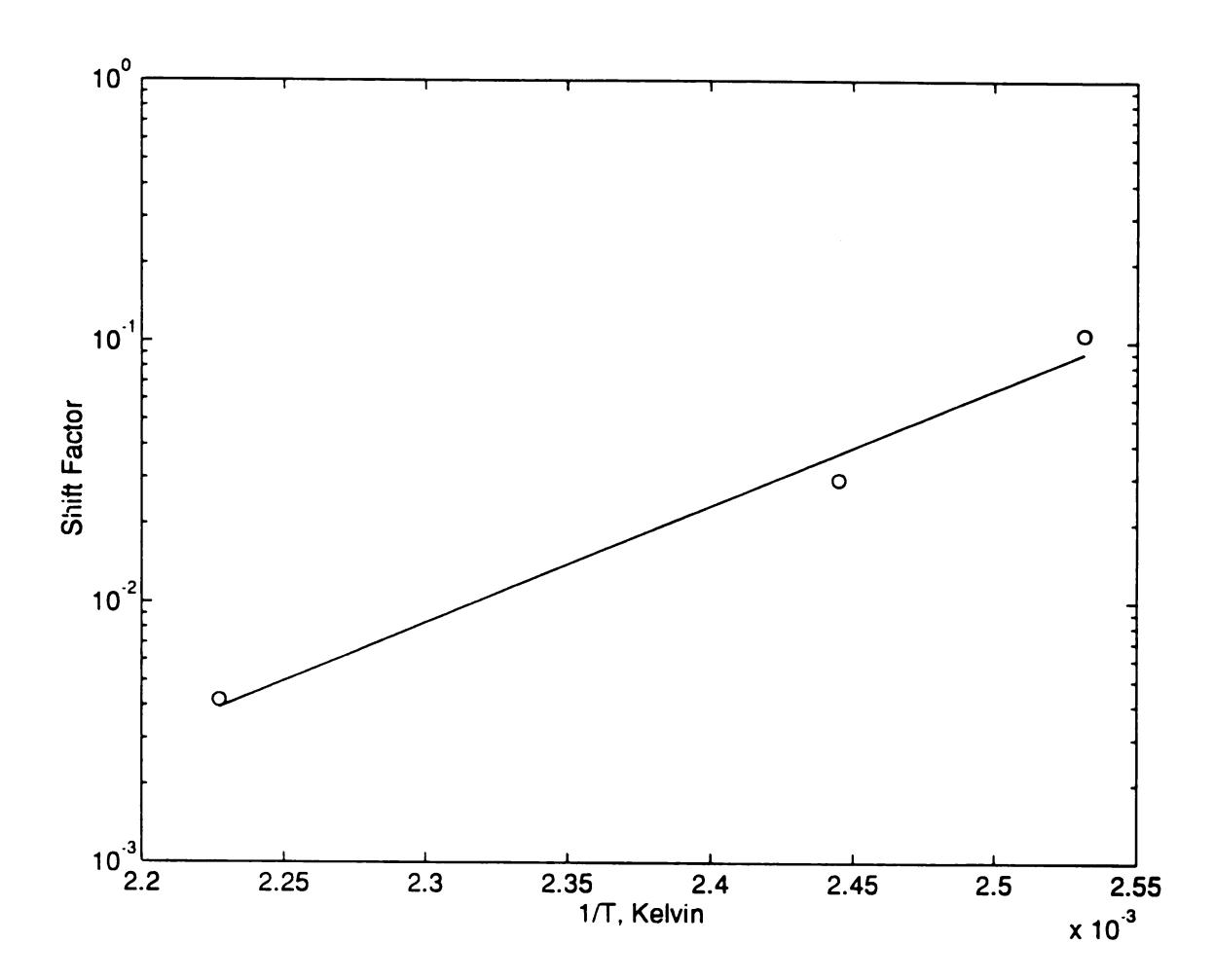


Figure 6. Arrhenius plot of shift factor for U-750 binder (T_{ref} = 93°C, Activation energy = 85 KJ/gmol).

pressure setting were averaged to yield one curve. Figure 7 shows each curve plotted on the same axis. In Figure 7 as well as all subsequent plots of pressure vs. fiber volume fraction, the data markers represent actual data points and the lines are the best fit to the Batch and Macosko model described earlier. The model selection is discussed in section 4.1. Each curve is seen to follow roughly the same pattern, but a trend of "trailing off" is seen, wherein the pressure transients for the mat stacks subjected to lower pressures are shifted to the right in the higher-pressure (non-Hookean) regime. This result was explained upon close examination of the force transients (Figure 3) by the discovery that the platen closing speed begins decreasing shortly before the platens stop altogether. During the period of platen slowing, the pressure continues to build up rapidly. Since the pressure builds rapidly even though the platens have slowed, the slope in the pressure / fiber volume fraction Consider curve increases. experimental runs: one done with a high maximum pressure, the other with a low maximum pressure. In the experimental run with a higher maximum pressure, the platens would not begin slowing at the same pressure as in the low-pressure run. Therefore, at that pressure, the run with the lower maximum pressure will have a higher slope, which is seen as a "trailing off" effect. Any other differences among the curves is attributed to experimental error and variation of the mats within the roll. It was concluded that the maximum pressure setting little effect the has on consolidation

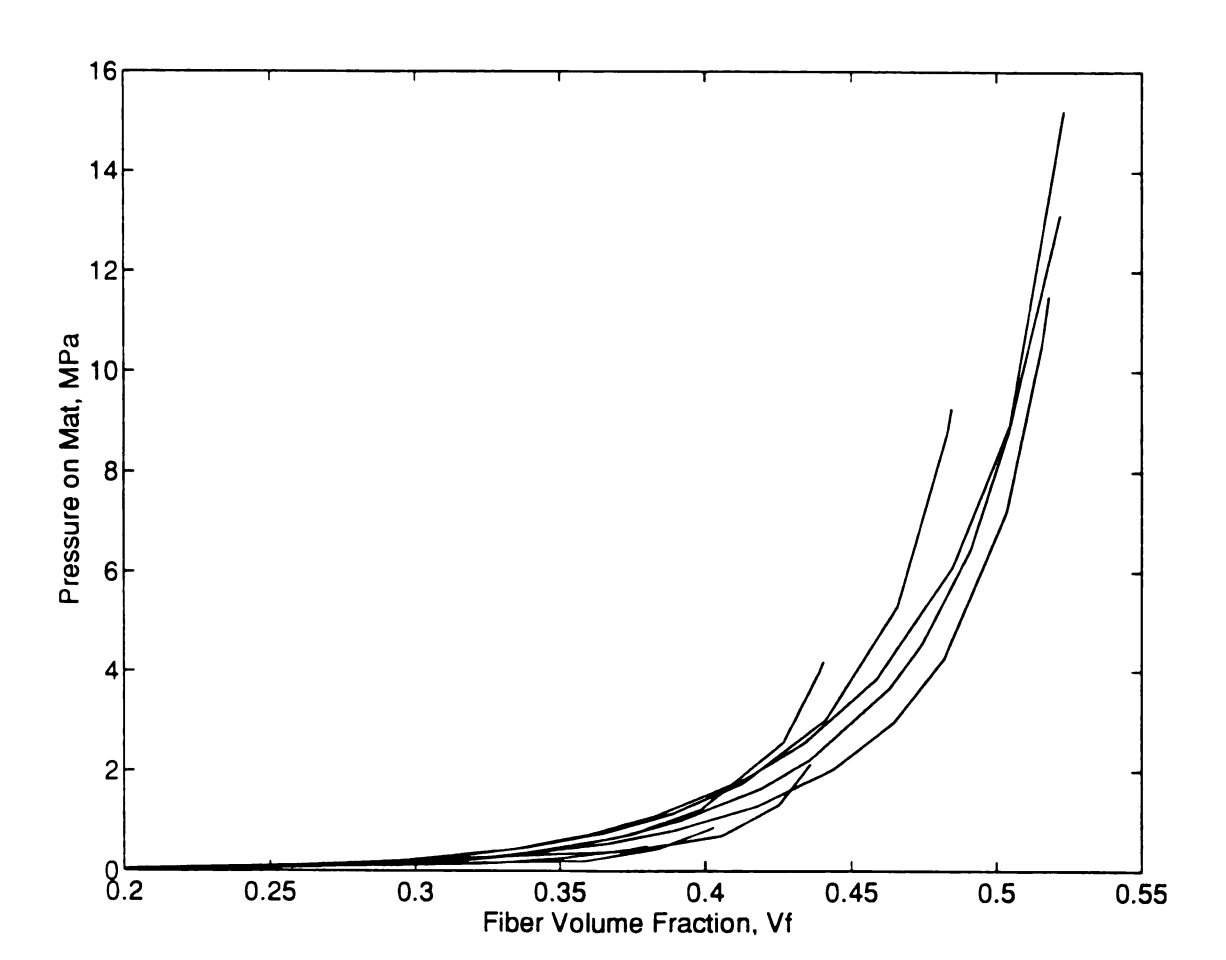


Figure 7. Effect of increasing maximum pressure on consolidation behavior of an eight-ply stack of U-750 at 93.3°C.

characteristics.

3.2.2. U-816 Consolidation Results

The next set of experiments was a study of consolidation characteristics of the U-816 mats. These mats were studied for purposes of comparison to the U-750 mats only. The binder in the U-816 mats is not thermoformable, so any changes observed in the consolidation must not be the effect of changing binder viscosity. The effect of closing rate on consolidation of U-816 mats was not considered in this study. Four experimental runs were done for each set of preforming conditions, and the four runs were averaged. The four resulting plots of pressure vs. fiber volume fraction are shown on the same axes in Figure 8. The variations seen in each curve are fairly small and are attributed to mat-to-mat variations and experimental error. One can conclude from this set of experiments that temperature does not have an effect on the consolidation behavior of mats without a thermoformable binder.

3.2.3. U-750 Consolidation Results

Next, the consolidation behavior of the mats with the medium solubility binder was considered. Unlike the low solubility binder mats, the binder in this case is thermoformable, so much different behavior was expected. Four experimental runs were performed at each temperature and closure rate and averaged, for a total of 16 sets with four

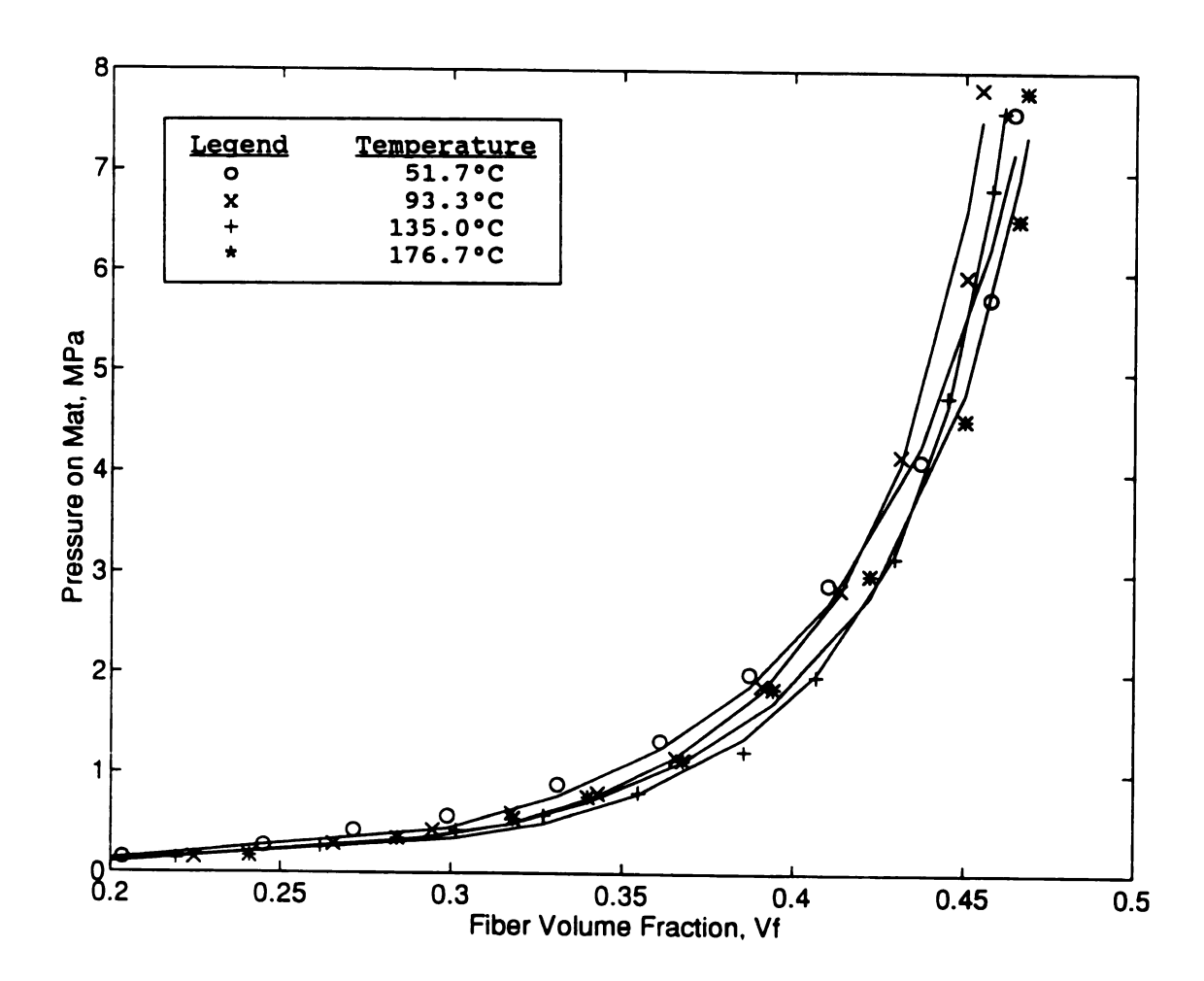


Figure 8. Consolidation behavior of an eight-ply stack of U-816 at 0.85 mm/sec.

runs each. The resulting plots of pressure vs. fiber volume fraction are shown in Figures 9-16.

Examination of Figures 9-16 reveal several trends in compressive behavior of the mat with both temperature and closing rate. As temperature increases at a constant closing speed (Figures 9-12), the curves are shifted to the right, which indicates that less force is required to achieve a certain fiber volume fraction, and the maximum amount of fiber packing is increased. The shape of the curves remain about the same in most cases, so the mechanism of compression and packing is probably unchanged. At the highest closing rate, however, increasing the temperature has an erratic effect on the curves. Some of this may be due to the high platen closing speed: the recorder cannot go fast enough, and the pressure builds up so fast that the pressure transient looks more like a vertical line than a curve. It may also be the result of binder shear-thinning, which is discussed in the next paragraph. The slope of the line in the Hookean region is decreased with increasing temperature, which is due to the decreasing stiffness of the mat with decreasing binder viscosity.

In compression experiments similar to those in this study, Kim et. al. [10] studied the effect of increasing platen closure rate on compressibility of dry 0/90 plain weave cloth (the temperature was not specified). Using closing speeds of 0.008 mm/sec, 0.033 mm/sec, and 0.083 mm/sec, it was observed that the consolidation curve moved to the left with

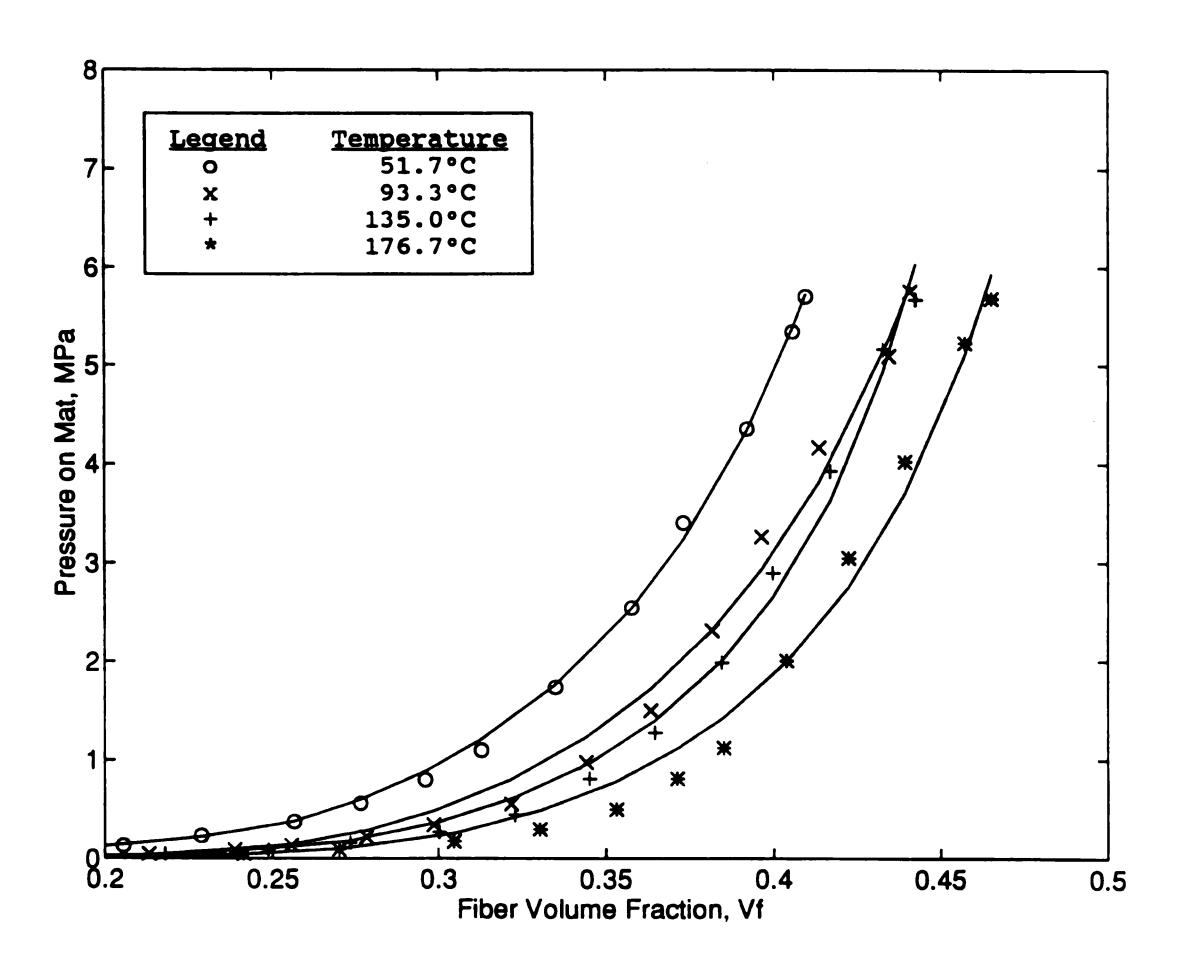


Figure 9. Consolidation behavior of an eight-ply stack of U-750 at 0.02 mm/sec.

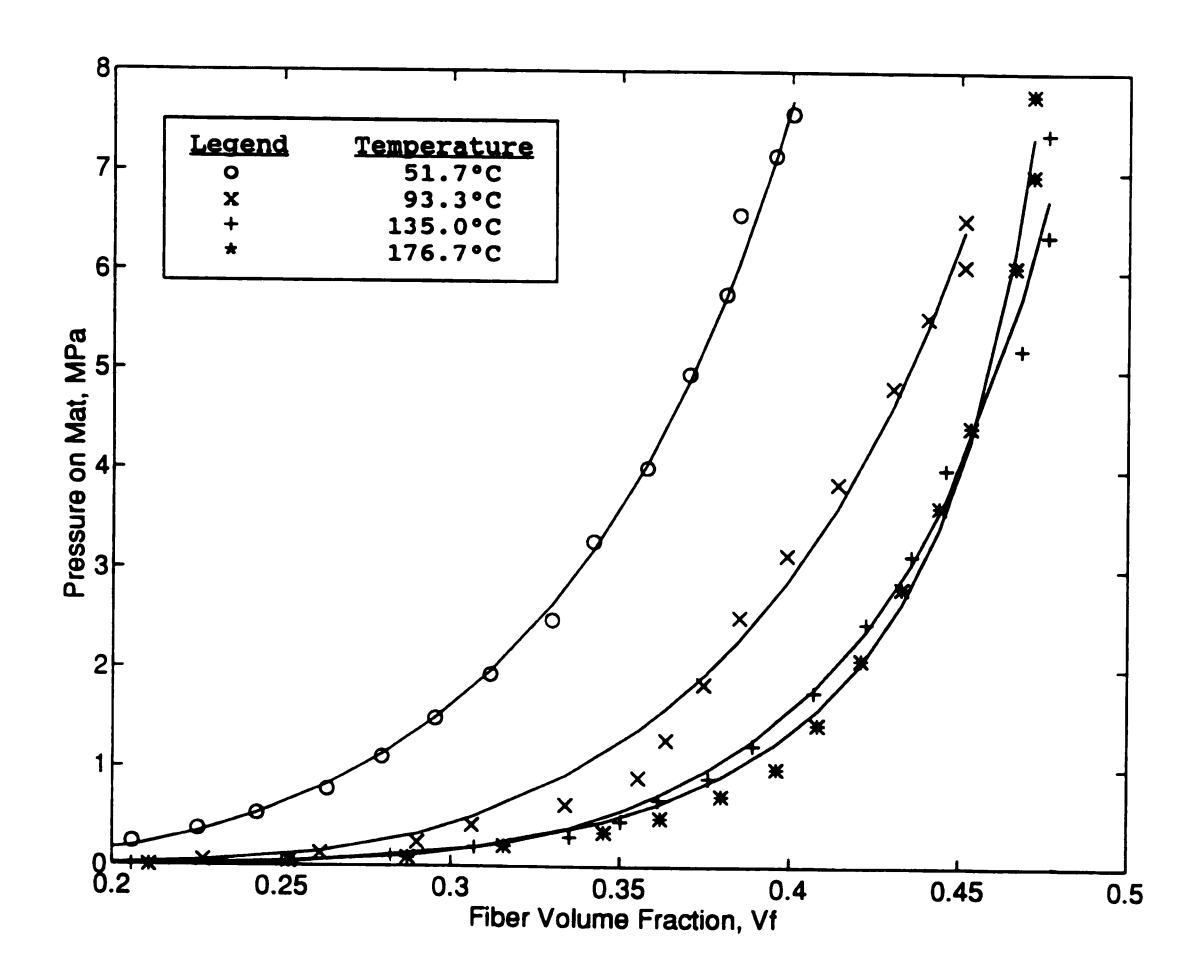


Figure 10. Consolidation behavior of an eight-ply stack of U- 750 at 0.15 mm/sec.

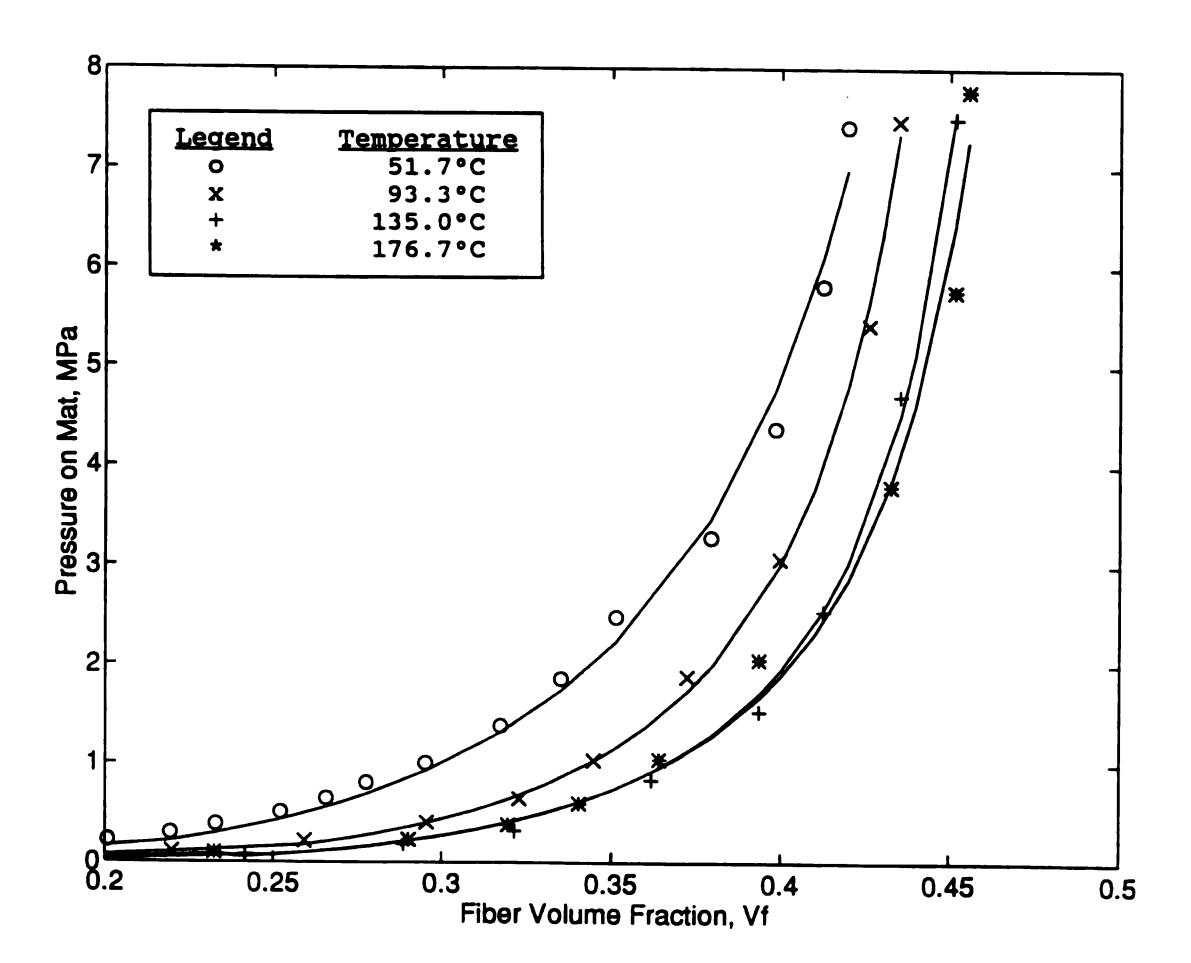


Figure 11. Consolidation behavior of an eight-ply stack of U- 750 at 0.85 mm/sec.

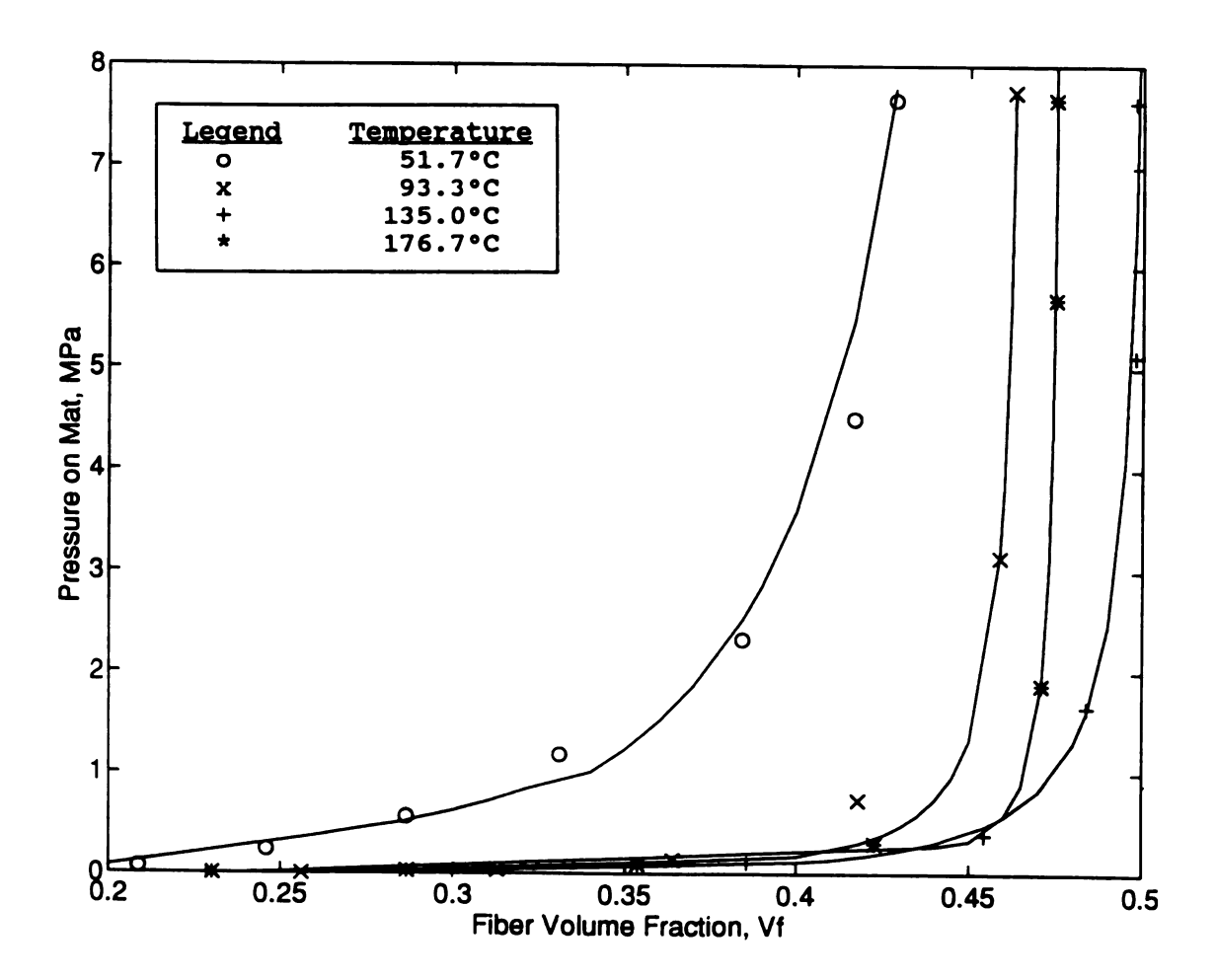


Figure 12. Consolidation behavior of an eight-ply stack of U- 750 at 2.00 mm/sec.

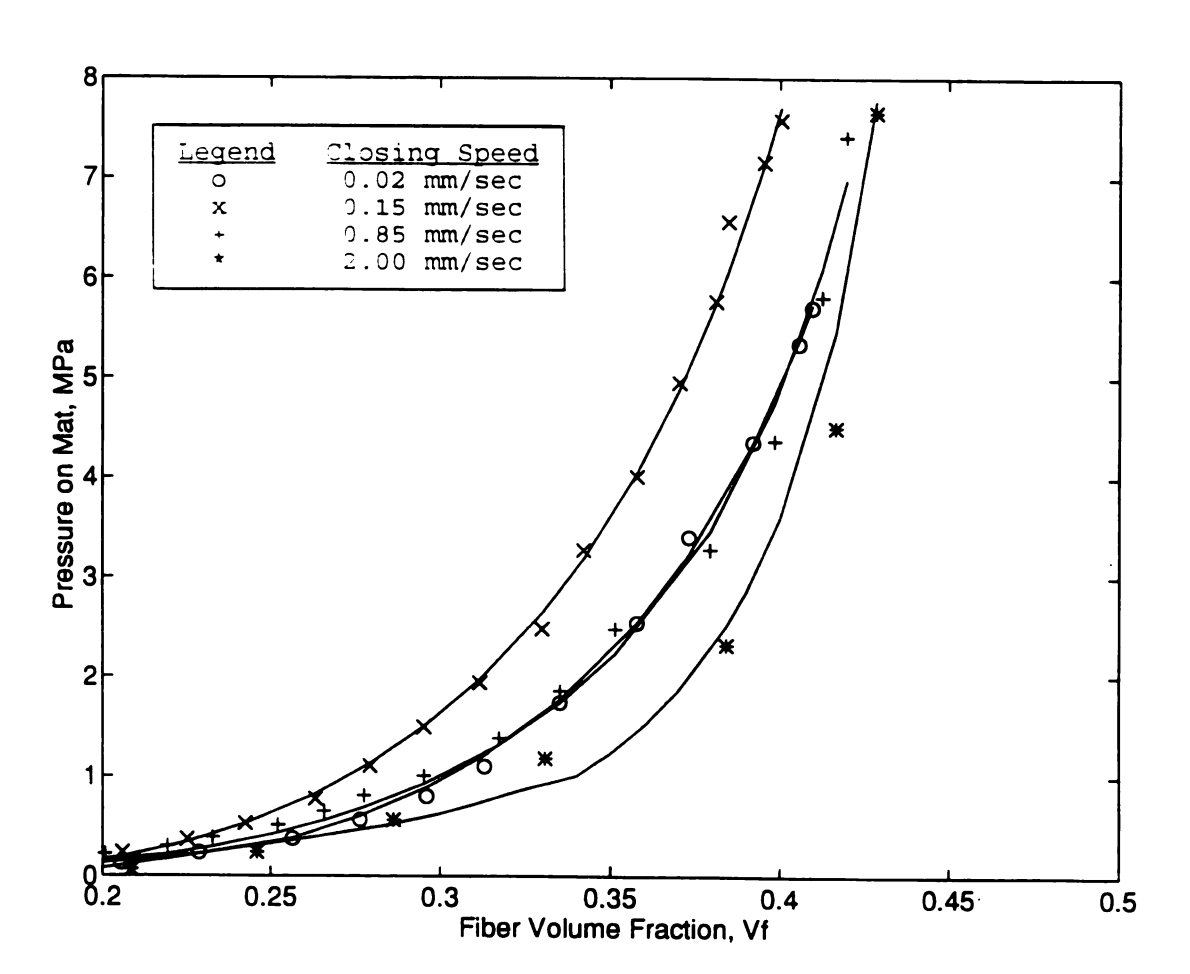


Figure 13. Consolidation behavior of an eight-ply stack of U-750 at 51.7°C.

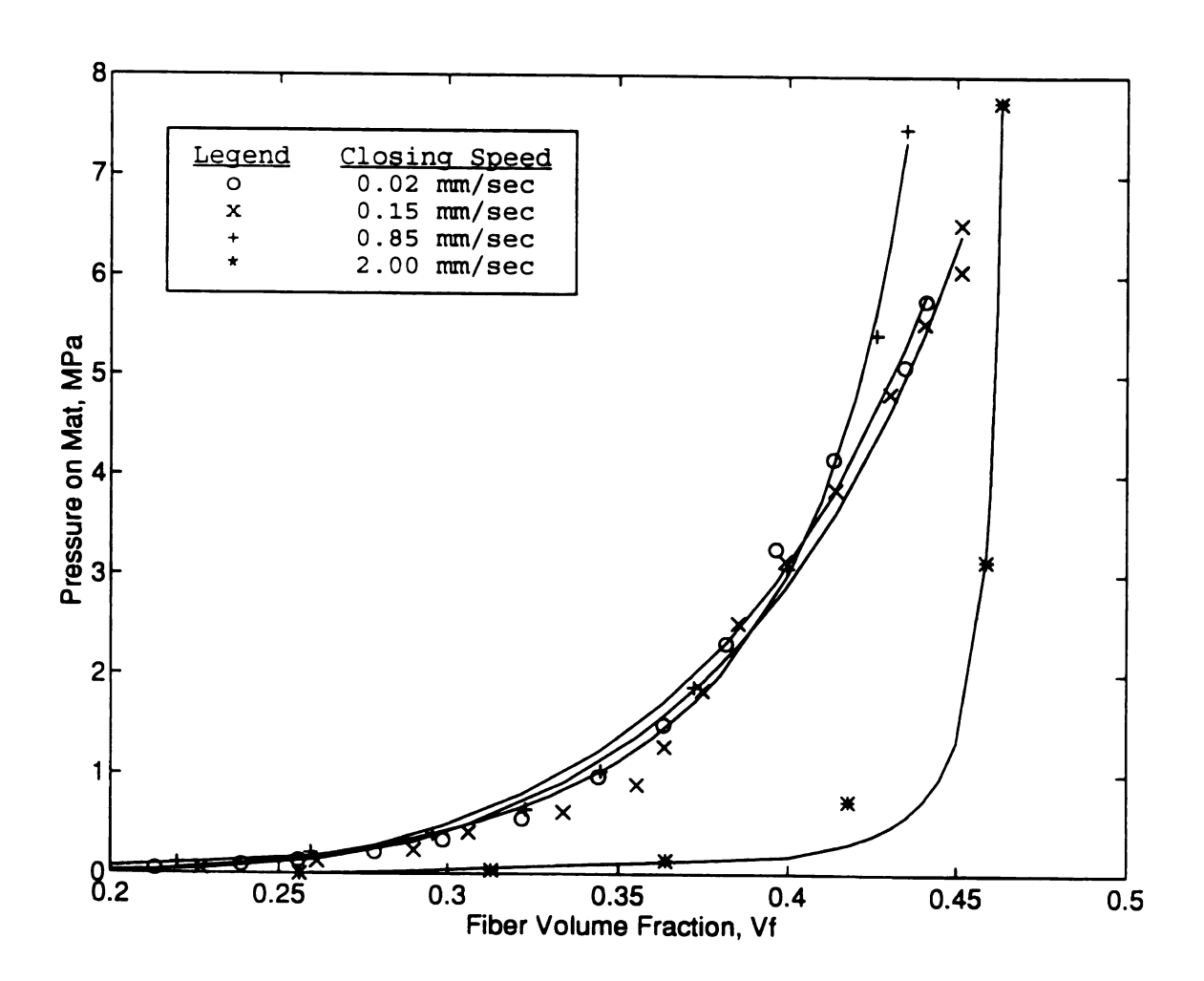


Figure 14. Consolidation behavior of an eight-ply stack of U-750 at 93.3°C.

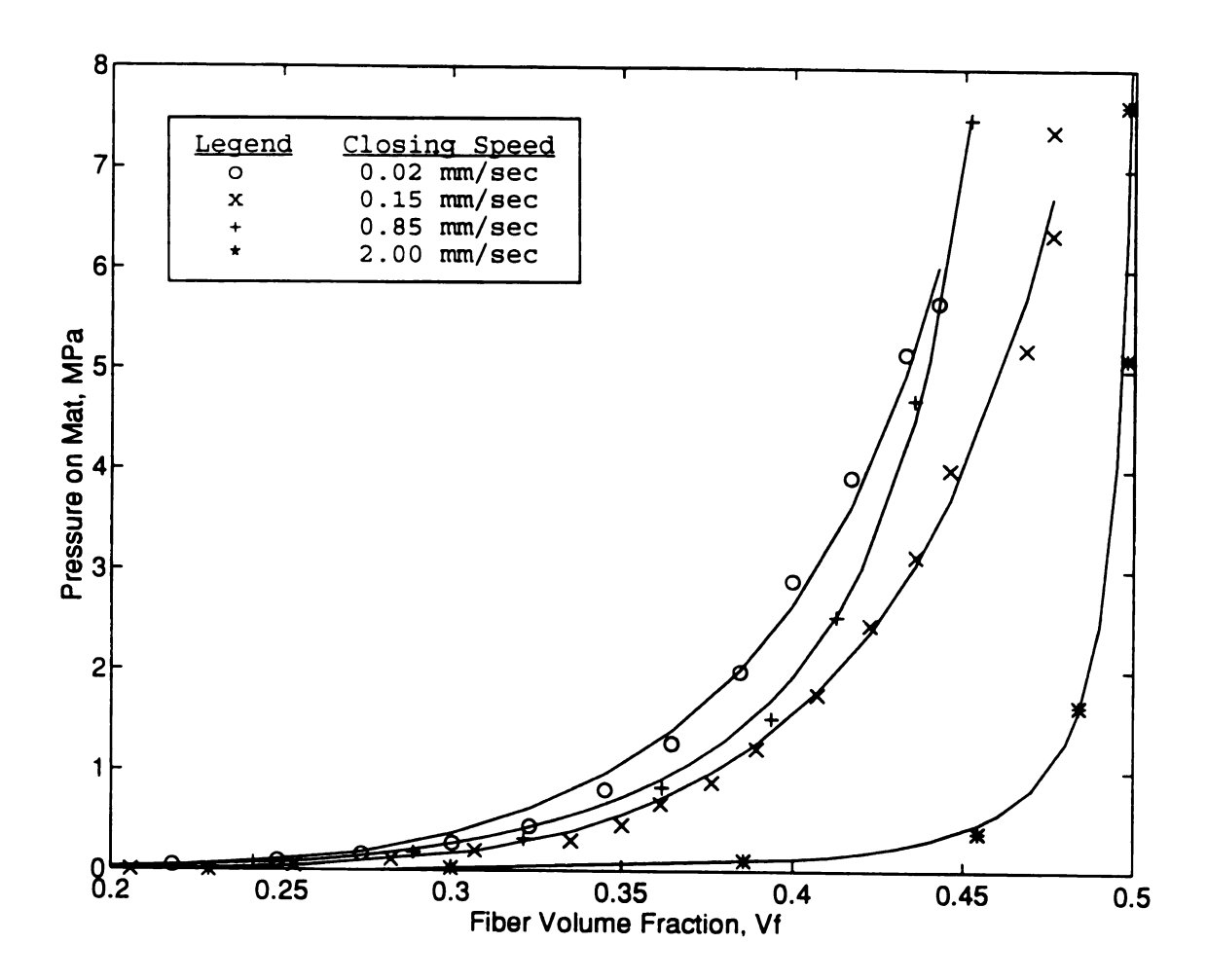


Figure 15. Consolidation behavior of an eight-ply stack of U-750 at 135.0°C.

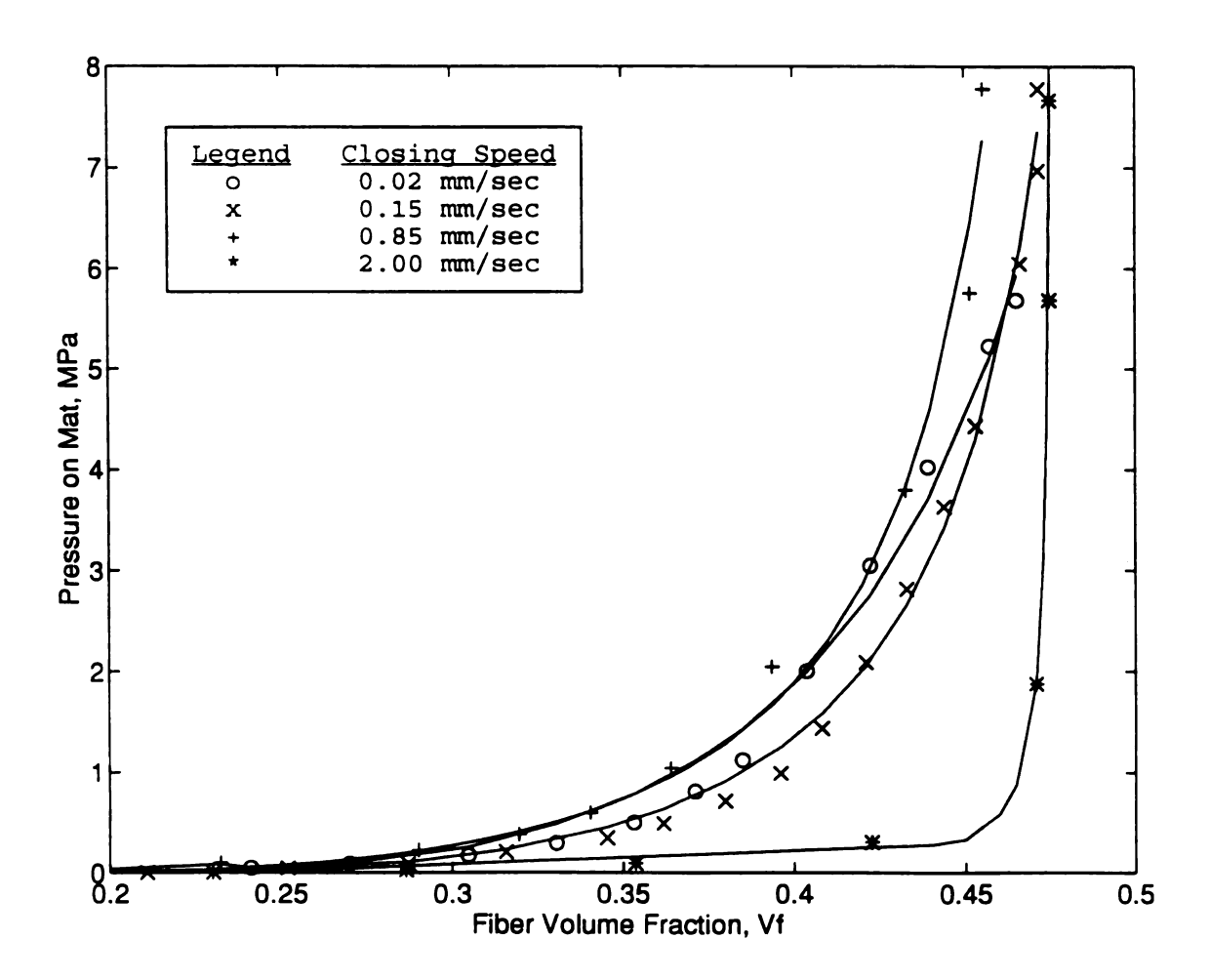


Figure 16. Consolidation behavior of an eight-ply stack of U-750 at 176.6°C.

increasing closing speed. It was postulated that a slower closing speed allowed more time for fiber rearrangement and thus required less force to compress the fibers. Similarly, Piechowski and Kendall [13] observed that lower closing speed (comparing closing speeds of 0.21 mm/sec and 1.27 mm/sec) allowed pressure reductions during compression, the amount of which was dependent on the number of layers in the mat and on platen temperature. It was suggested that the increased time the mat is on the heated platens (at low closing speed) lets the binder soften more and thus requires less force. The results of these other studies partially conflicts with observations from the current study; here it is seen in Figures 13-16 that at moderate closing speeds (0.15 mm/sec to 0.85 mm/sec), the force required for compression does increase with increasing closing speed, and the compression curve lies farther to the left. However, at high closing speeds (2.00 mm/sec) the fiber mat acts like an aligned fiber system; the pressure is considerably lower during compaction and the pressure rises very rapidly after network formation. In these runs, the fiber tows may have been forced past each other to the point of network formation just by the momentum of the closing platen. Another possible explanation of this is the shear-thinning behavior of the binder. Although the shear rate sustained by the binder within the mat is not measurable, it is possible that at high closing rates it is sufficient to lower the binder viscosity enough that the fibers can move more freely. If so, the increased freedom of the fibers would

lead to reductions in pressure, delay the formation of the fiber network, and allow the fibers to reach maximum packing with little force. Each of the consolidation curves of increasing closing speed at constant temperature come closer together near the maximum fiber volume fraction, which indicates that the closing rate has a smaller effect on packing. As in the case of increasing temperature, the slope of the Hookean region of the curves decreases with increasing closure rate, although the decrease is smaller among the three slower closing rates. It should also be pointed out that it has been observed in the literature [13] that the pressure variability in consolidation of random mats is higher at higher speeds. This was observed in the current study as well, as the highest amount of experimental scatter was in the runs at the highest closing speed. However, the curves in this study were moved significantly to the right at temperature, especially at the knee in the curve.

The study conducted by Davis and McAlea [14] showed the first stage of a GMT load/deformation curve (Figure 17) to be similar to those for fiber mats alone. Their void reduction and resin squeeze-out section exhibited the same behavior as the U-750 mats observed in the current study. The first section of GMT consolidation was brief if few voids were formed in the heating and lofting stage, and ended when all voids had been eliminated and the resin and fibers began flowing as one. The similarity in the appearance of Davis and McAlea's curve to one from the current study (compare the

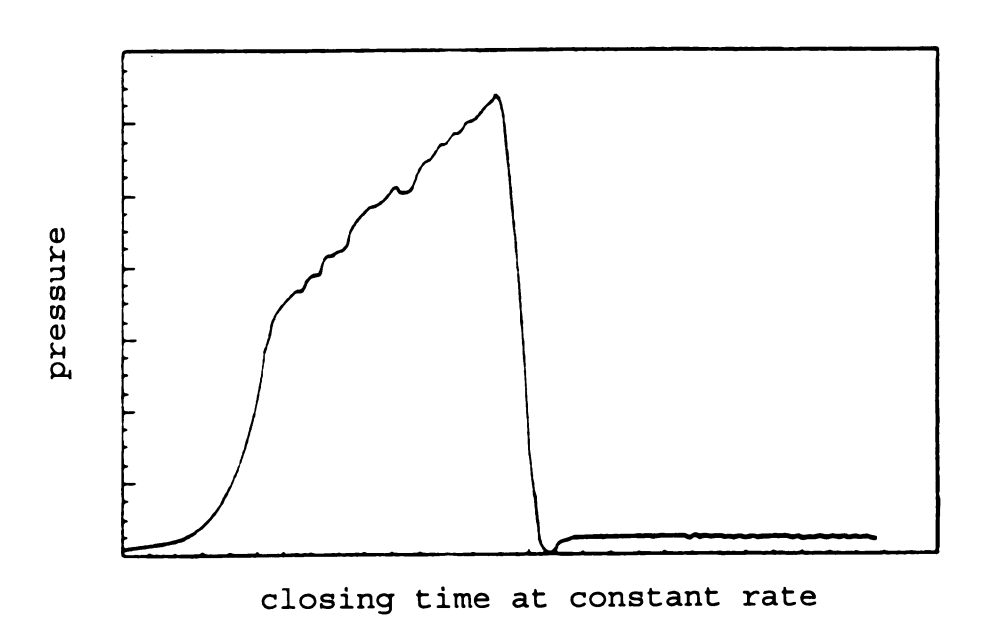


Figure 17. Consolidation behavior of glass mat-reinforced thermoplastics (GMTs) [14].

first stage of Figure 17 to Figure 9) shows that the presence alone of a filling material (such as thermoplastic matrix or a binder) should have no effect on the nature of the fiber deformation unless all the voids have been filled.

3.3. Mat Relaxation Results

Relaxation studies were performed on stacks of both U-750 and U-816 mats, on the U-816 only as a control experiment. The results of the relaxation study on U-750 are summarized in Table 2 and the results of the study on U-816 are in Table 3.

Table 2. Relaxation of U-750 glass mat stacks, %.

	0.85 mm/sec	2.00 mm/sec		
51.7°C	32.4	46.8		
93.3°C	11.6	10.9		
135.0°C	32.4	31.2		
176.7°C	34.7	34.8		

Table 3. Relaxation of U-816 glass mat stacks, %.

	0.85 mm/sec	2.00 mm/sec		
51.7°C	76.2	77.2		
93.3°C	75.2	78.2		
135.0°C	77.4	74.2		
176.7°C	72.3	73.3		

Table 2 shows that above the binder melting point, relaxation increased as temperature increased. This agrees with the findings of Piechowski and Kendall [13], who in a statistical study determined that temperature effects are responsible for 94% of the relaxation variability, and that relaxation increased as platen temperature increased. The relaxation runs done just near the U-750 binder melting point were quite high, but lower than the relaxation of the U-816 mats, probably due to the binder beginning to soften and become sticky. An increase in closure rate was found to have little effect on relaxation of the U-750 stack, which was expected since the binder should have the same viscosity at the start of the actual relaxation process regardless of the speed at which it was compressed, since at the start of relaxation there is no shear applied to the mat. This result agrees with the findings of Piechowski and Kendall, who found that closing speed effects are small and thus may be set to optimize other parameters in the thermoforming process such as compression force. The increase in relaxation with increasing temperature was suggested by Piechowski and Kendall to possibly be due to the binder melting and flowing to the bottom of the mat stack, but the binder was observed on the top edges in the scanning electron microscopy experiments done on similarly processed mats (see section 3.3). The increase in relaxation with increasing temperature may be due to the greater ability of the fibers to move about and spring back to their original positions when the viscosity of the binder is

lowered. The U-816 mats showed little variation in relaxation with either temperature or closing speed. This was expected since the binder in the U-816 mats was not thermoformable.

3.4. Scanning Electron Microscopy Study Results

A photomicrograph of undeformed U-750 mat is shown in Figure 18; the magnification is 20x and the fiber volume fraction of the mat is about 0.03. Photomicrographs with the same magnification of the preformed U-750 mats are shown in Figures 19a-19h. The fiber volume fractions in the preformed mats are 0.41 - 0.49.

The photomicrographs of the preformed plaques show striking differences in the plaques as both temperature and closing speed are increased. The tows all show some degree of flattening, which is higher at higher temperatures and lower closing speeds. In addition to the flattening effect, one can also see that as the temperature and closing speed are increased, the binder flows between the fiber tows more and penetrates the tows to wet out the individual fibers more. Some breakage of the fibers can also be observed, although it is not seen in each photomicrograph, and no apparent trend for breakage is seen.

Observation of the photomicrographs may help explain some of the different trends seen in the consolidation characteristics of the mats. The rapid formation of the fiber network (rapid rise in pressure) at 51.7°C may be due to the unmelted blobs of the binder keeping the fiber tows from

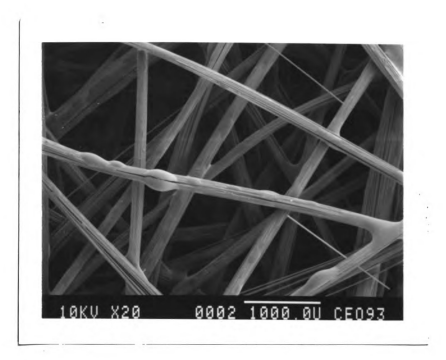


Figure 18. Scanning electron micrograph (20x magnification) of undeformed U-750 ($V_{\rm f}=$ 0.03).



Figure 19a. Scanning electron micrograph (20x magnification) of U-750 consolidated at 0.02 mm/sec and 51.7°C ($V_{\rm f}$ = 0.41)



Figure 19b. Scanning electron micrograph (20x magnification) of U-750 consolidated at 2.00 mm/sec and 51.7°C (V_t = 0.43)



Figure 19c. Scanning electron micrograph (20x magnification) of U-750 consolidated at 0.02 mm/sec and 93.3°C (V_t = 0.44)



Figure 19d. Scanning electron micrograph (20x magnification) of U-750 consolidated at 2.00 mm/sec and 93.3°C (V_f = 0.46)



Figure 19e. Scanning electron micrograph (20x magnification) of U-750 consolidated at 0.02 mm/sec and 135.0°C (V, = 0.44)



Figure 19f. Scanning electron micrograph (20x magnification) of U-750 consolidated at 2.00 mm/sec and 135.0°C ($V_r = 0.49$)



Figure 19g. Scanning electron micrograph (20x magnification) of U-750 consolidated at 0.02 mm/sec and 176.7°C ($V_r=0.47$)



Figure 19h. Scanning electron micrograph (20x magnification) of U-750 consolidated at 2.00 mm/sec and 176.7°C (V_f = 0.47)

moving around one another and packing. As the platen temperature is increased above the binder melting point, the viscosity of the binder is lowered, which in turn allows more movement of the fiber tows within the preform. Thus, the formation of the fiber network is delayed and a buildup of pressure comes later. The most significant delay in network formation is between 51.7°C and 93.3°C for each closing speed, which supports the hypothesis that unmelted binder blobs play a role in network formation. The flattening of the fiber tows is greater at higher temperatures and slower closing speeds, which indicates that tows flatten more when the individual fibers have more time to move about and are moving through binder of reduced viscosity. The increase in final fiber volume fraction with increasing temperature may be partly because as the fiber tows flatten more, they pack more closely together.

To gain some more insight as to what happens to the individual fiber tows in the center of the mat stack, as well as at the edge, an "apparent number" of fiber tows was calculated. Using the scale located near the bottom of each photomicrograph, the widths of each fiber tow can be determined. The widths of the fiber tows are summarized in Table 4. Figure 20 shows the trends in fiber tow thickness with increasing temperature and closing speed. Assuming that the fibers are flattened to a roughly rectangular shape and that the cross-sectional area of the individual fiber tows remains roughly constant, the apparent number of fiber tows

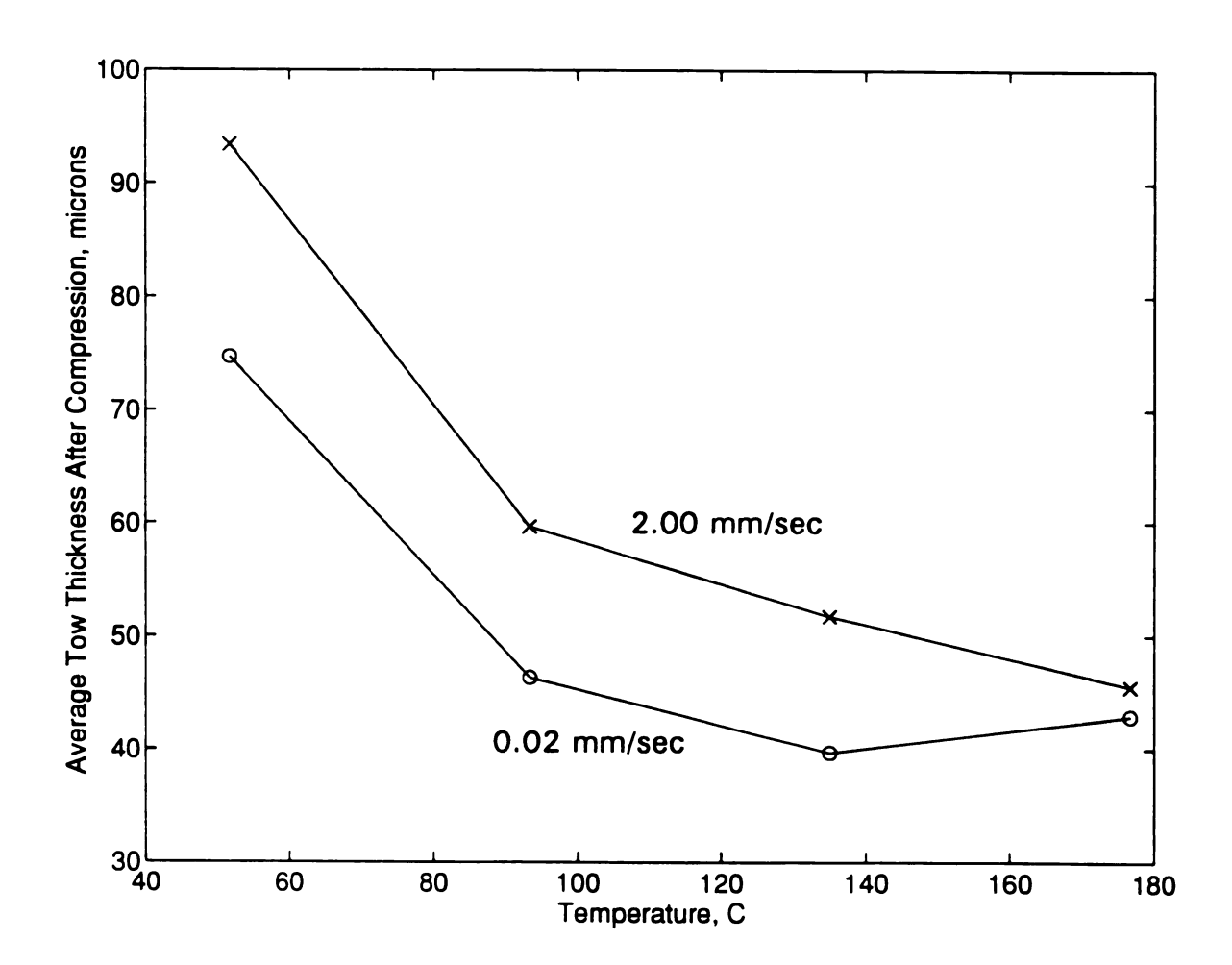


Figure 20. Average thickness of U-750 fiber tows after consolidation.

Table 4. Average width of U-750 fiber tows after thermoforming.

	0.02 mm/sec	2.00 mm/sec		
51.7°C	292 μm	233 μm		
93.3°C	470	365		
135.0°C	549	421		
176.7°C	508	47 9		

making up the thickness of the plaque was found by dividing the known final mat thickness by the tow thickness determined from the photomicrographs. Also, knowing the original, undeformed size of the fiber tows, the apparent number of tows in the mat thickness at the point of network formation can be calculated. Comparison of the apparent number of tows in the mat thickness before and after pressure is applied can show more about the behavior of the mat during the preforming process. The number of fiber tows in the plaque thickness at the point of network formation (start) and at maximum compression (end) is summarized in Table 5 (see appendix A for a sample calculation). The expected result of this study is that the apparent number of fiber tows should be the same in However, examination of Table 5 shows some all cases. interesting results. At the lowest temperature, the apparent number of fiber tows in the plaque thickness is higher at the start of compression than at the end. The photomicrographs of these two runs (Figure 19a and Figure 19b) show that the

Table 5. Apparent number of U-750 fiber tows in mat thickness before and after consolidation.

	0.02 mm/sec start end change		2.00 mm/sec start end change			
51.7°C	56.6	41.8	-14.8	45.4	32.1	-13.3
93.3°C	47.2	62.2	+15.0	35.6	43.6	+8.0
135.0°C	45.8	72.5	+26.7	33.7	49.3	+15.6
176.7°C	42.0	68.2	+26.2	32.6	59.3	+26.7

binder in these systems is not completely melted. This again suggests that at the low temperatures, the binder plays a role in keeping the fiber tows apart: the unmelted binder holds the fiber tows and prevents them from moving or settling. Thus, the network is formed quickly and some of the load is carried by unmelted blobs of the binder. The extra thickness added to the fiber tows by the solid binder accounts for the higher apparent number of tows in the plaque thickness at the start of compression. At full compression, the unmelted binder is pressed into the mat and the tows are flattened somewhat, which reduces the apparent number of tows.

The apparent number of fiber tows at full compression is highest at high temperatures and slower closing rates, when the amount of flattening is also greatest. This may be due to a 'piling' effect associated with flattening of the fiber tows: when the tows flatten, they spread out and contact other tows, which keeps the mat thickness relatively high. Another possible explanation for the increasing apparent number of

tows before and after compression is non-uniformity of the amount of flattening throughout the mat. For example, if the fiber tows in the center of the mat are much thicker than the tows at the edges, a much higher than expected apparent number of fiber tows would be calculated. Because the apparent number of fiber tows is much higher for the mats compressed at slower closing speeds, the tow thickness in the center of the mat must be greater. The mats compressed at higher speeds have smaller apparent numbers of fiber tows, so they must have more even flattening throughout the mat.

Use of SEM may also help explain the relaxation phenomena described in Section 3.3. Recall that relaxation increased with increasing temperature above the binder melting point. Below the melting point, as seen in Figures 19c-19h, the unmelted blobs of binder help keep the fiber tows apart and prevent adhesion between fiber tows; when the pressure is released the mat simply springs back. The photomicrographs show the flattening effect to vary in the same way as the relaxation: increasing with increasing temperature increasing a small amount with increasing closure rate. The elastic storing of increased energy associated straightening and flattening the fiber tows coupled with the greater fiber mobility may be the reason for the observed relaxation behavior.

CHAPTER 4

MODELLING

4.1. Model Selection

Of all the models described in previous sections, the two which were considered were Gutowski's and Batch and Macosko's. The reason for this is that those two are based on theories of deformation, while the other models are empirical. A drawback to Gutowski's model is that he developed his model for aligned carbon fiber systems; in this work the fibers are random. Recall that in Gutowski's model, the three parameters are A, V_o , and V_m ; in Batch and Macosko's model, the parameters are $K_o,\ h,\ V_o,\ \text{and}\ V_{\infty}.$ To determine which of the two was the model of choice, all of the data sets for the medium solubility binder mat compression experiments were fit to both models. A non-linear regression routine in the mathematics software package IMSL and the spreadsheet SuperCalc were used to determine the best-fit parameters of each model for each different set of processing conditions. The results of that parametric study are summarized in Table 6 and Table 7. As can be seen from a perusal of the tables, Gutowski's model can be made to fit the data for random fiber mats; however, the fits are not very good and at least one of the parameters loses physical meaning (see Table 6; note that V, in some instances is greater than 1). Batch and Macosko's model fit the data much better, which was expected since the model was developed to predict behavior of both aligned and random glass mats.

From this parametric study it was concluded that Batch and Macosko's model was the model of choice for these experiments. The Batch and Macosko model parameters for the U-816 mats and for the varied maximum pressure experiments are summarized in Table 8 and Table 9, respectively.

Table 6. Gutowski model parameters, U-750 mat.

Rate,mm/s	T, °C	As	Vo	Va
0.02	51.7	1.60	0.14	1.15
0.02	93.3	1.02	0.17	1.10
0.02	135.0	0.50	0.17	0.94
0.02	176.7	0.31	0.20	0.92
0.15	51.7	3.68	0.13	1.27
0.15	93.3	1.39	0.19	1.13
0.15	135.0	0.19	0.21	0.87
0.15	176.7	0.04	0.21	0.71
0.85	51.7	1.05	0.12	1.08
0.85	93.3	0.086	0.17	0.73
0.85	135.0	0.024	0.17	0.66
0.85	176.7	0.064	0.18	0.74
2.00	51.7	0.033	0.16	0.65
2.00	93.3	1.20e-5	0.23	0.51
2.00	135.0	3.30e-5	0.23	0.54
2.00	176.7	2.79e-7	0.23	0.49

Table 7. Batch & Macosko model parameters, U-750 mat.

Rate, mm/s	T, °C	Ko	h	Vo	V∞	Vf,cont
0.02	51.7	3.25	0.48	0.16	0.53	0.24
0.02	93.3	2.62	0.35	0.20	0.58	0.26
0.02	135.0	2.19	0.35	0.20	0.54	0.25
0.02	176.7	2.01	0.36	0.22	0.56	0.28
0.15	51.7	2.79	0.41	0.14	0.53	0.20
0.15	93.3	2.89	0.34	0.21	0.59	0.27
0.15	135.0	2.84	0.41	0.24	0.55	0.31
0.15	176.7	1.16	0.40	0.21	0.51	0.28
0.85	51.7	1.98	0.58	0.12	0.50	0.21
0.85	93.3	2.20	0.60	0.17	0.48	0.27
0.85	135.0	1.52	0.55	0.18	0.49	0.27
0.85	176.7	2.00	0.60	0.18	0.49	0.29
2.00 2.00 2.00 2.00 2.00	51.7 93.3 135.0 176.7	4.60 1.24 0.95 0.76	0.78 0.80 0.70 0.89	0.18 0.24 0.28 0.24	0.46 0.49 0.50 0.48	0.34 0.40 0.40 0.43

Table 8. Batch and Macosko model parameters, U-816 mat.

Rate,mm/s	T,°C	Ko	h	Vo	V∞	Vf,cont
0.85	51.7	3.13	0.68	0.16	0.53	0.30
0.85	93.3	2.77	0.69	0.16	0.50	0.31
0.85	135.0	2.35	0.73	0.15	0.50	0.31
0.85	176.7	2.39	0.69	0.15	0.52	0.30

Table 9. Batch and Macosko model parameters, varied maximum pressure on U-750 mat.

Max P, MPa	Ko	h	Vo	V∞	Vf,cont
0.55	0.99	0.74	0.18	0.45	0.32
0.89	1.20	0.82	0.19	0.44	0.36
2.10	2.40	0.84	0.21	0.46	0.39
4.24	1.43	0.67	0.18	0.47	0.31
9.92	1.17	0.47	0.19	0.52	0.27
11.74	1.17	0.47	0.20	0.55	0.28
13.83	2.80	0.48	0.22	0.58	0.31
16.14	2.28	0.46	0.23	0.56	0.31
18.43	1.75	0.43	0.21	0.60	0.29

After determining which model to use, the sensitivity of the parameter values to changing curve shapes was considered. In the Batch and Macosko model, an increase in h (increased randomness of the mat) increases the transitional fiber volume fraction and causes the fiber volume fraction to reach its maximum value at lower pressure. As h approaches 1, the pressure / fiber volume fraction curve approaches a straight line with slope Ko. Ko has no effect on the transition to non-Hookean behavior, but an increase in Ko increases the slope of the curve in the Hookean region and increases the pressure required to reach the same volume fractions. An increase in V_o delays the point at which pressure first begins to build up, and an increase in V_{∞} increases the maximum amount of packing of the fibers. It was also observed that two curves, one with an increase in h and a proportionally smaller decrease in V. from the other, may look nearly identical. This was noted as

a possible cause of error in determining the proper values of the parameters.

4.2. Comparison of Model to Experimental Data

Examining Table 7 shows some trends for the medium solubility binder mat in the parameters with increasing temperature and platen closing rate. As temperature increases, K_o decreases, V_o and $V_{f,cont}$ increase, and V_{∞} and h are largely unchanged. The trends of K_o , V_o , and $V_{f,cont}$ are consistent with observations from the plots, but those in h and V_{∞} are not. However, it is probable that the h / V_{∞} interaction within the model is responsible for this. As platen closing rate is increased, K_o and V_{∞} decrease, h and $V_{f,cont}$ increase, and V_o remains mostly unchanged. The increase in h, which especially prominent at the highest closing rate, is probably due to the increased freedom of the fiber tows to move around during the consolidation process at high closing rates. fibers are packed close together quickly at the high rates, but as soon as the limit is reached the pressure rises very rapidly. The result of this much steeper pressure transient is an increase in the random-like behavior of the mat and an increase in h. The trend inconsistent with the observations in this case is that of V_{∞} . The model predicts a decrease in V_{∞} , but on the graphs this is not seen; rather, there is close agreement between the highest fiber volume fractions among the three lower closing rates and a small increase in the highest closing rate. This is likely due to the steep increase in the

pressure during the fastest closing speed runs. The steep transient makes it appear that the maximum fiber volume fraction has already been reached instead of going to V_{∞} asymptotically.

With the U-816 mats, the plot shows four lines which are nearly the same; the model parameters show the same. Except for a small decrease in K_o , especially with the first run, the parameters all stay at about the same value. The decrease in K_o is probably due to experimental error and mat variations. The lack of variation was an expected result, since the binder did not melt or otherwise experience a transition.

The experiments in which the maximum pressure setting was increased are also largely as expected. V_0 and $V_{f,cont}$ were largely unchanged, which was expected since the maximum pressure was outside of the Hookean regime in all cases and therefore should not have had an effect on them. V_∞ increased as was also expected because of the "trailing-off" effect near the highest volume fraction reached. The decrease in h is due to the increase in the amount of compression after the Hookean regime, which makes the fiber system appear less random. There was an irregular increase in Ko with increasing maximum pressure, which was not an expected result, since the press closed in the same way during each experimental run in the low fiber volume fraction region, so the Hookean behavior should not have been affected. This result may have been due to experimental error in reading the pressure transients or slight differences within the mats.

CHAPTER 5

SUMMARY AND CONCLUSIONS

The consolidation and relaxation behavior of continuous strand random glass mats with binders were studied over temperatures from 51.7°C to 176.7°C and closing speeds from 0.02 mm/sec to 2.00 mm/sec. Scanning electron microscopy (SEM) was used to examine sections of the mats after consolidation. The conclusions drawn from this study were:

- 1. Lowering the binder viscosity by increasing the temperature decreases the pressure required during compression, delays the formation of the fiber network, and increases the final fiber volume fraction. These effects are consistent with the observation (using SEM) of increased flattening of fiber tows at higher temperatures.
- 2. At moderate closing speeds, the compaction pressure on the mat is increased with increasing speed. This observation is also consistent with SEM observations of decreased fiber tow flattening at higher closing speeds. At the highest observed closing speeds, however, the compaction pressure is decreased significantly, and the mat behaves more like an aligned fiber system.
- 3. Relaxation of a fiber mat is increased by increasing the processing temperature because the decreased binder viscosity allows easier motion of the fiber tows, which in turn makes it easier for the tows to spring back into shape.
 - 4. Changing the closing speed at constant temperature has

no effect on relaxation. This is presumably because the binder is not experiencing any shear at the start of the relaxation process and thus would have the same viscosity regardless of the closing speed.

- 5. Scanning electron microscopy is a useful tool in examining processed glass mats. Fiber tow flattening, which is greatest at high temperatures and low closing speeds, can be seen using SEM. The flattening is related to some of the trends observed in the compaction curves of the mats.
- 6. The model proposed by Batch and Macosko fits the consolidation curves fairly well. A number of trends are seen in the model parameters with variations in temperature and closing speed.

CHAPTER 6

RECOMMENDATIONS

6.1. Recommendations for This Work

- 1. Use a computer to do the data collection. Data collection for the consolidation process in these experiments done by recording pressure and platen gap height continuously on a strip chart recorder. The data points must then be read from the chart, which is a slow process of matching points from the two lines drawn on a chart and measuring their position above a baseline as accurately as possible with a ruler and the eyes of the Experimental error is inherent in the process. Also, at higher platen closure rates, the pressure reaches the preset maximum very fast, so the pressure line looks more like a spike than a curve and it is very hard to read accurately. Both of these problems could be solved by the addition of a computer data collection process. By reading voltages from the pressure transducer and the potentiometer directly into a computer's memory, more accurate data can be obtained much more quickly.
- 2. Add an environmental chamber to the press. Heating the mat stacks to platen temperature is currently done simply by leaving the stack in the press with the top platen just touching the top of the stack for several minutes. However, it is unlikely that the entire stack would reach platen temperature this way, since some heat transfer would occur between the sides of the stack and the ambient air. The amount

of error due to this fact is unknown, but the problem could be eliminated by adding an environmental chamber to the press, thus heating ambient air to platen temperature as well as the ambient air.

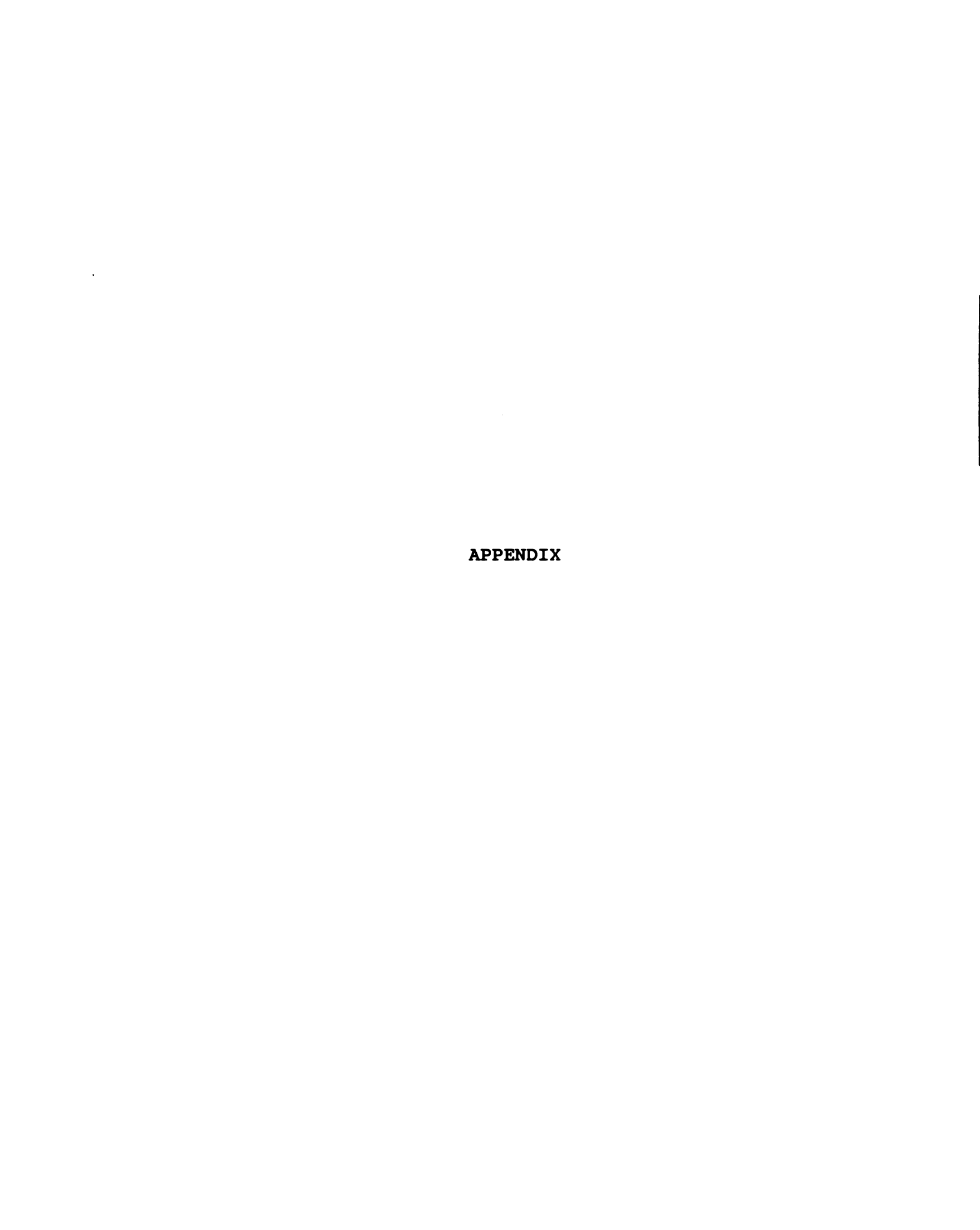
3. Perform more repetitions for a better average. The experimental results presented in this work are all the averages of three or more runs. Because of mat-to-mat variations and variations within the mat itself, some of the repeated experimental runs showed considerable differences in pressure/volume fraction data, and a better picture of the true behavior of the mats may have required more repetitions of the same runs. With the addition of the computer for data collection, the tedious task of reading the strip charts would be eliminated, and a better statistical average of the runs would be obtained.

6.2. Recommendations for Future Study

1. A binder washout study. The soluble binder used in the glass mats is intended to be dissolved and washed away by the resin during an injection molding process. The dissolution of the binder can cause viscosity gradients in the resin, which may affect the properties of the finished part. The selected preforming conditions, since they have an effect on the behavior of the binder within the preform, may affect the rate of dissolution and washout of the binder during injection molding. Thus, a study of the effect of preforming conditions on the rate of binder washout should be carried out and added

to this work. A simple injection molding process in which resin without any initiator is injected into a mold containing a random fiber mat and collected in 20 mL samples as it flows out is suggested. The resin would then be tested for viscosity and the amount of binder present in the samples would be determined by comparison with a calibration curve of weight percent binder in the resin versus viscosity. Several differently thermoformed mats should be tested to determine if thermoforming conditions have any effect on the rate of binder washout.

2. Establish a database of information for binder selection. Since it has been shown in this work that the viscosity of a thermoplastic binder can affect the processing of a random glass mat, it may be possible to select a binder to optimize the processing conditions. In an industrial thermoforming process, it is desirable to reduce the equipment sizes and heating requirements of the process to reduce costs and to reduce cycle time to produce as many parts as possible quickly. If a particular binder could be found that was of optimum viscosity to reduce pressure at some temperature, it would be of great industrial importance. It is suggested that a study of random glass mats containing many different kinds of binders be tested similarly to this study to establish a database of information to be used in binder selection.



APPENDIX A

SAMPLE CALCULATIONS

1. Calculation of V_f from platen gap data

Fiber volume fraction can be defined as the ratio of the volume of the fibers to the volume of the mat, i.e.,

$$V_{\rm f} = \frac{\it fiber volume}{\it mat volume} = \frac{\it fiber mass}{\it fiber density} \over \it (mat area) (mat thickness)$$

(Note: "mat area" means the area of the mat on which the compressive force acts.) Since the fibers constitute 92% of the weight of the mat and thickness can be factored out, the expression above can be rewritten:

$$V_{\rm f} = \frac{\text{0.92(total mass of plies)}}{\text{mat area}} * \frac{1}{\text{mat thickness}}$$

Fiber density = 2.54 g/cm^3 Mat Area = $10.3 \text{ cm x } 10.3 \text{ cm} = 106.1 \text{ cm}^2$ Mass of Plies = 38.50 gThen

$$V_{f} = \frac{(0.92) (38.50 \ g)}{(2.54 \frac{g}{cm^{3}}) (106.1 \ cm^{2})} * \frac{1}{mat \ thickness, cm} = \frac{0.134}{mat \ thickness, cm}$$

Or

$$V_f = \frac{1.34}{\text{mat thickness,mm}}$$

2. Calculation of apparent number of fiber tows in U-750 mat thickness

In the case of consolidation at 0.02 mm/sec and 200 F, examination of the photomicrographs before and after the consolidation process yields the following data:

Average thickness of undeformed fiber tow = 166.5 μm Average thickness of fiber tow after consolidation = 46.3 μm

From the experimental procedure, the following data is obtained:

Average platen gap height at point where fibers begin to carry a load (V_o) = 7.86 mm = 7860 μm

Average platen gap height at maximum pressure (V_a) = 2.88 mm = 2880 μm

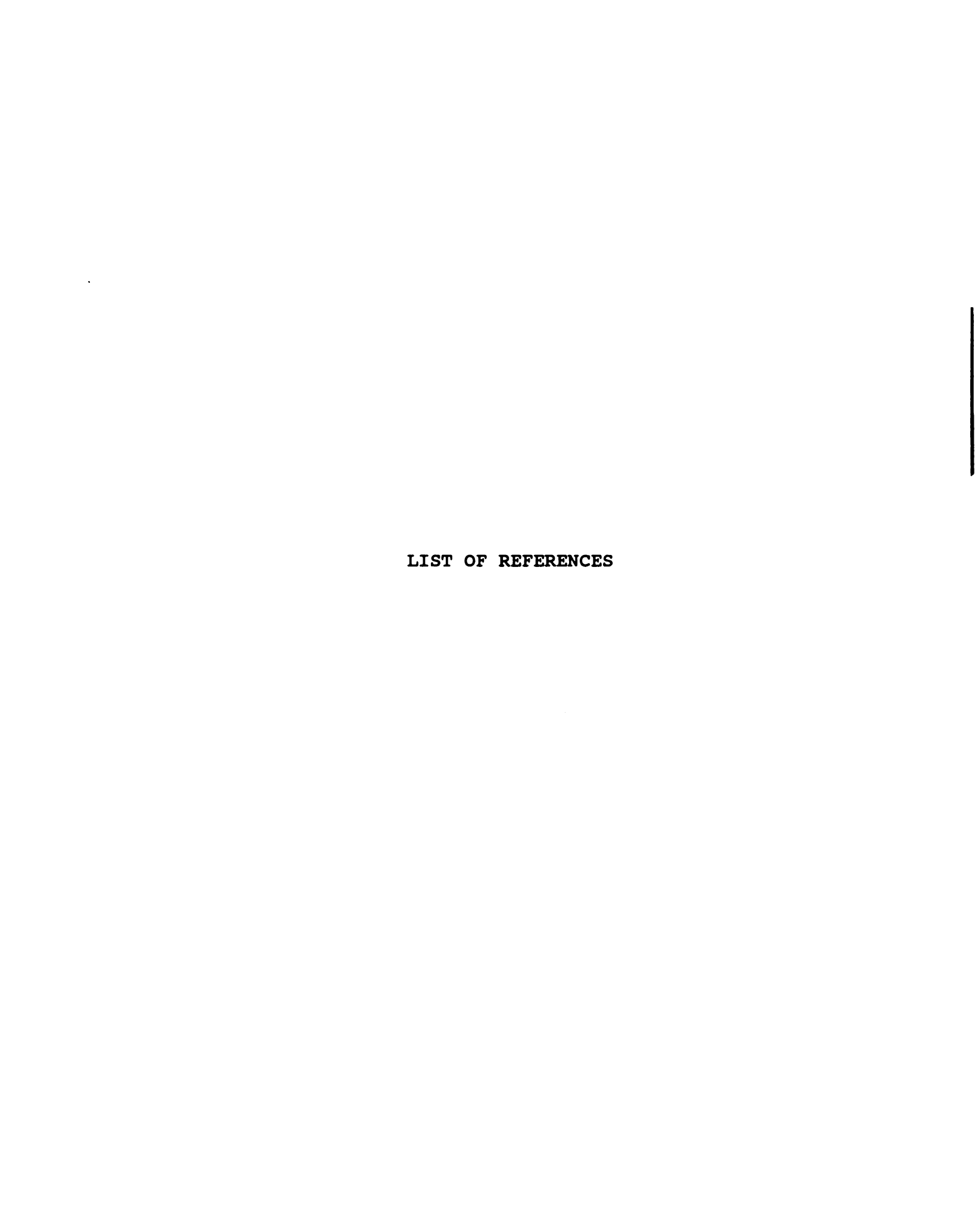
Assuming that the fiber mat can be modelled as having a solid thickness of fiber tows,

At Va,

$$\frac{2880 \, \mu m}{mat} * \frac{tow}{46.3 \, \mu m} = 62.3 \, \frac{tow}{mat}$$

At Vo

$$\frac{7860 \mu m}{mat} * \frac{tow}{166.5 \mu m} = 47.2 \frac{tow}{mat}$$



LIST OF REFERENCES

- 1. Gutowski, T.G. "A Resin Flow / Fiber Deformation Model for Composites." SAMPE Quarterly, Vol. 16, No. 4, pp. 58-64 (1985).
- 2. Gutowski, T.G., J. Kingery, and D. Boucher. "Experiments in Composites Consolidation: Fiber Deformation." Proceedings of the Society of Plastics Engineers 44th Annual Technical Conference, Boston, May 1986, pp. 1316-1320.
- 3. Gutowski, T.G., Z. Cai, J. Kingery, and S.J. Wineman. "Resin Flow / Fiber Deformation Experiments." SAMPE Quarterly, Vol. 17, No. 4, pp. 54-58 (1986).
- 4. Gutowski, T.G., Z. Cai, S. Bauer, D. Boucher, J. Kingery, and S. Wineman. "Consolidation Experiments For Laminate Composites." *Journal of Composite Materials*, Vol. 21, No. 7, pp. 650-669 (1987).
- 5. Gutowski, T.G., Morigaki, and Z. Cai. "The Consolidation of Laminate Composites." *Journal of Composite Materials*, Vol. 21, No. 2, pp. 172-188 (1987).
- 6. Gutowski, T.G., and Z. Cai. "The 3-D Deformation Behavior of a Lubricated Fiber Bundle." *Journal of Composite Materials*, Vol. 26, No. 8, pp. 1207-1237 (1992).
- 7. Gutowski, T.G., and G. Dillon. "The Elastic Deformation of Lubricated Carbon Fiber Bundles: Comparison of Theory and Experiments." *Journal of Composite Materials*, Vol. 26, No. 16, pp. 2330-2347 (1992).
- 8. Batch, G., and C. Macosko. "A Model for Two-Stage Fiber Deformation in Composite Processing." 20th International SAMPE Technical Conference, September 27-29, 1988.
- 9. Hou, T.H. "A Resin Flow Model for Composite Prepreg Laminate Process." Proceedings of the Society of Plastics Engineers 44th Annual Technical Conference, Boston, May 1986, pp. 1300-1305.

- 10. Kim, Y.R., S.P. McCarthy, and J.P. Fanucci.
 "Compressibility and Relaxation of Fiber Reinforcements
 During Composite Processing." *Polymer Composites*, Vol. 12,
 No. 1, pp. 13-19 (1991).
- 11. Taylor, D.W. <u>Fundamentals of Soil Mechanics</u>. New York: John Wiley and Sons (1948).
- 12. Knight, J.C., and K. Jayaraman. "Consolidation Behavior of Continuous Strand Random Glass Mats with Binders." Society of Automotive Engineers Technical Paper Series, Paper # 930176. Presented at SAE International Congress and Exposition, March 1, 1993.
- 13. Piechowski, L.J., and K.N. Kendall. "Factors Affecting the Compressibility and Relaxation of Thermoformable Continuous Strand E-glass Mat." Proceedings of the 9th Annual ASM/ESD Advanced Composites Conference and Exposition, Dearborn, MI, pp. 215-222 (1993).
- 14. Davis, S.M., and K.P. McAlea. "Isothermal Rheological Characterization of Glass Mat Reinforced Thermoplastics." Chapter in <u>Mechanics of Plastics and Plastic Composites</u>, ed. V.K. Stokes. New York: ASME, pp. 227-242 (1989).
- 15. Trevino, L., K. Rupel, W.B. Young, M.J. Liou, and L.J. Lee. "Analysis of Resin Injection Molding in Molds with Preplaced Fiber Mats. I: Permeability and Compressibility Measurements." *Polymer Composites*, Vol. 12, No. 1, pp. 20-29 (1991).
- 16. Bird, R.B., R.C. Armstrong, and O. Hassager. <u>Dynamics of Polymeric Liquids</u>, <u>Volume 1</u>. New York: John Wiley and Sons, 1987.

AICHIGAN STATE UNIV. LIBRARIES
31293010431983